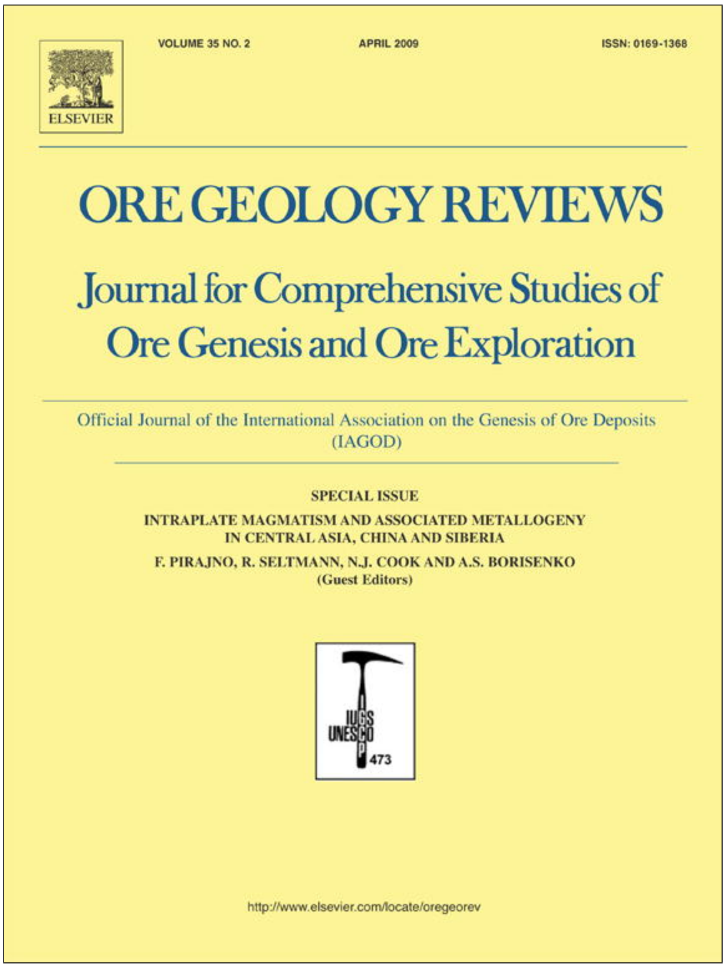
VOLUME 35 NO. 2
APRIL 2009
ISSN: 0169-1368
ELSEVIER
ORE GEOLOGY REVIEWS
Journal for Comprehensive Studies of Ore Genesis and Ore Exploration
Official Journal of the International Association on the Genesis of Ore Deposits (IAGOD)
SPECIAL ISSUE
INTRAPLATE MAGMATISM AND ASSOCIATED METALLOGENY IN CENTRAL ASIA, CHINA AND SIBERIA
F. PIRAJNO, R. SELTMANN, N.J. COOK AND A.S. BORISENKO
(Guest Editors)
IUGS
UNESCO
473
http://www.elsevier.com/locate/oregeorev

Ore Geology Reviews 35 (2009) 137–154

Contents lists available at ScienceDirect

Ore Geology Reviews

journal homepage: www.elsevier.com/locate/oregeorev

Intraplate magmatism and oceanic plate stratigraphy of the Paleo-Asian and Paleo-Pacific Oceans from 600 to 140 Ma

I. Yu. Safonova

Institute of Geology and Mineralogy SB RAS, Koptyuga ave. 3, Novosibirsk, 630090, Russia

A R T I C L E I N F O

Article history:
Received 24 March 2008
Received in revised form 16 September 2008
Accepted 16 September 2008
Available online 23 September 2008

Keywords:
Basalt
Geochemistry
Mantle plume
Sedimentary rocks
Accretionary complex
Paleo-Asian ocean
Paleo-Pacific ocean

A B S T R A C T

This paper reviews localities of intraplate basalts of the Paleo-Asian and Paleo-Pacific Oceans, which occur as fragments of former oceanic islands, seamounts and plateaus in accretionary complexes of Altai-Sayan, Russian Far East and Southwest Japan. Special emphasis is given to their relationships with associated rocks of oceanic plate stratigraphy (OPS), major and trace element chemistry and criteria for their identification in structurally complex orogenic belts. Accretionary complexes (ACs) host the Late Neoproterozoic–Early Cretaceous OPS units of the two paleo-oceans, which have a number of features in common: i) similar succession of oceanic sediments (pelagic chert – hemipelagic terrigenous slope facies – reef carbonates); ii) intraplate basalts occur at the bottom of the sedimentary sections and are usually overlain by a carbonate "cap"; iii) typical OIB-type chemistry of basalts is characterized by LREE–Nb–Ti enrichment. There is a 100 Ma time gap in the evolution of the oceanic intraplate magmatism, which is probably a result of our insufficient knowledge of other ACs of Central Asia. The study of intraplate magmatism and OPS of paleo-oceans is very important because it is an integral part of the study of orogenic belts incorporating many commercially valuable mineral deposits. Identification of intraplate OPS units should be based on a combination and mutual correlation of geological, lithological and geochemical features of basalts and their associated sediments. OPS units, both magmatic and sedimentary, provide a full geological record of the evolution of paleo-oceans from their opening, through subduction and formation of accretionary complexes, and finally to their closure accompanied by active tectonics, orogeny and ore mineralization.

1. Introduction

Recognizing oceanic basalts of intraplate origin – oceanic islands, seamounts and plateaus – as elements of oceanic plate stratigraphy (OPS after Isozaki et al., 1990) is important for reconstructing the evolution of paleo-oceans, continental growth and formation of OPS-related mineral deposits. It is generally accepted that oceanic intraplate magmatism is related to mantle plumes, which are imaged as columns of heated material ascending from the lower mantle (e.g., Morgan, 1971; Maruyama, 1994; Hofmann, 1997, Montelli et al., 2004; Nolet et al., 2007). The surface expressions of plume magmatism are hot spot or intraplate oceanic basalts (hereafter oceanic island basalts or OIB-type basalts), which presently occur as fragments in accretionary complexes of foldbelts formed in the place of former oceans (Sengör et al., 1993; Buslov et al., 2001; Safonova et al., 2004). The mode of geological occurrence, structural position, petrological and geochemical features of OIBs help us to reconstruct epochs of ocean opening and closure and accretion-related processes of continental growth.

Unlike oceanic crust rocks formed at spreading zones (i.e., ophiolites), oceanic island basalts incorporated in accretionary complexes or accretion-collisional belts provide a better record of the evolution of paleo-oceans and continental active margins, because: (i) they are better preserved during subduction due to their significant height and higher buoyancy compared to oceanic crust; (ii) sometimes they can block the subduction zone and thus enhance the accretion; (iii) it is possible to date the basalts by their associated sedimentary rocks, mainly carbonates and cherts; and (iv) OIB's are indicative of an intraplate geodynamic setting, which characterizes the main stage of ocean evolution (Dobretsov et al., 2004). Geochemistry of intraplate basalts and the associated sedimentary rocks allow us to follow the evolution of paleo-oceans from their initial opening recorded in riftogenic basaltic dikes possessing OIB-type geochemical affinities, through their maximal opening, recorded in basalt-sedimentary units of intraplate origin, up to their closure recorded in accretionary and collisional complexes. Petrologic study of intraplate volcanic rocks provides information about the physico-chemical conditions of the mantle which existed at the time of volcanism and allows evaluation of the environmental impact of volcanic eruptions. Structural position of OIB's and their relationship with the other members of OPS – pelagic (radiolarian-/ribbon/bedded chert), hemipelagic (siliceous shale, mudstone, carbonate breccia) and shallow-water carbonates (massive/bedded/reef limestone; Isozaki et al., 1990) – helps to understand mechanisms of accretion (e.g., Wakita, 2000) and subsequent

E-mail address: inna@uiggm.nsc.ru.

0169-1368/$ – see front matter © 2008 Elsevier B.V. All rights reserved.
doi:10.1016/j.oregeorev.2008.09.002

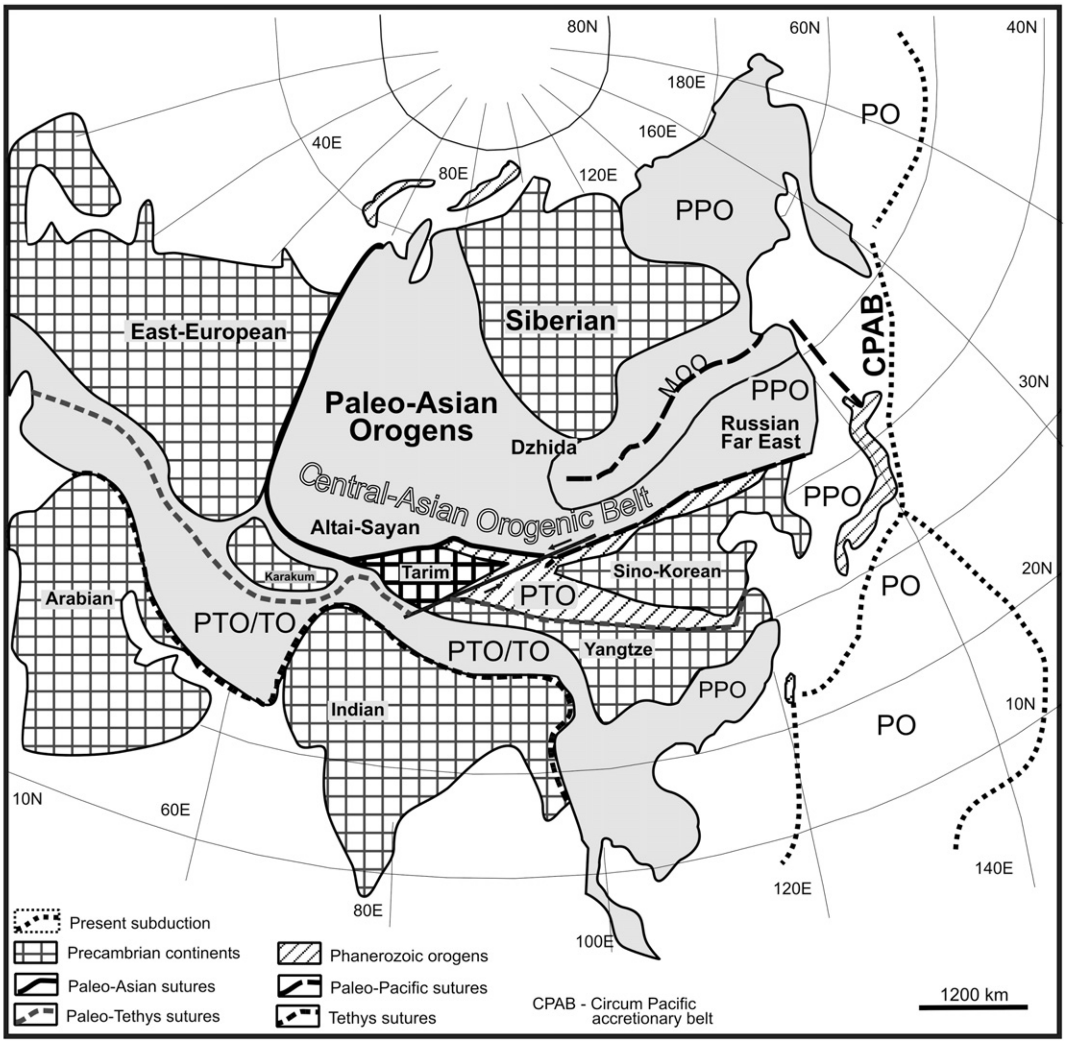

Fig. 1. Tectonic scheme of Asia showing main orogens formed in place of former oceans: PPO—Paleo-Pacific, PTO—Paleo-Tethys, TO—Tethys, PO—modern Pacific; MOO—Mongolian–Okhotsk orogenic belt (modified from Li, 2006).

formation of mineral deposits (Nakae and Komuro, 2005). Finally, identification of OIB is important for mantle plume modeling and global geodynamic paleo-reconstructions.

Worldwide, oceanic islands, seamounts and plateaus occur as slivers within accretionary wedges that faced former major oceans. The plume-related basalts of the Paleo-Asian Ocean are hosted by Cambrian to Carboniferous accretionary complexes of the Central Asian Orogenic Belt (e.g., Didenko et al., 1994; Jahn et al., 2000; Windley et al., 2007). The plume-related basalts of the Paleo-Pacific Ocean are hosted by the Permian to Cretaceous accretionary complexes of the Russian Far East (e.g., Kojima et al., 2000; Kirillova et al., 2002) and Southwest Japan (e.g., Sano and Kanmera, 1991; Kanmera et al., 1990; Isozaki et al., 1990; Kojima and Kametaka, 2000) (Fig. 1). The tectonic evolution and metallogeny of both oceans and their accretionary complexes are believed to be strongly influenced by plume events (e.g., Kovalenko et al., 1999; Dobretsov and Vernikovsky, 2001; Yakubchuk, 2004), which are better evidenced by magmatic rocks possessing OIB geochemical signatures and by OPS units.

The tectonic reconstructions on the Central Asian Orogenic Belt (e.g., Zonenshain, 1973; Sengör et al., 1993; Didenko et al., 1994; Yakubchuk, 2004), despite different approaches, typically considered its oceanic units as fragments of the large, long-living Paleo-Pacific Ocean (e.g., Maruyama et al., 2007). Dobretsov et al. (1995) alternatively interpreted the opening of the Paleo-Asian Ocean to be prior to the Paleo-Pacific opening and consequently considered oceanic units of the Central Asian Orogenic Belt as fragments of the Paleo-Asian Ocean. Recently, Li (2006) summarized that the Central Asian Orogenic Belt may have formed due to subduction of the Paleo-Asian Ocean and, the accretionary complexes of Russian Far East and Southwest Japan—due to the subduction of the Paleo-Pacific Ocean. Accordingly, in the present paper the Late Neoproterozoic–Paleozoic OPS units of the Central Asian Orogenic Belt (Transbaikalia and Altai-Sayan) will be related to the Paleo-Asian Ocean and the Mesozoic oceanic units of Russian Far East and Southwest Japan accretionary complexes to the Paleo-Pacific Ocean (Fig. 1).

The Central Asian Orogenic Belt is one of three giant metallogenic belts in the world—Tethyan, Paleo-Asian and Circum-Pacific (Hou et al., 2007). It was formed during the amalgamation of continental blocks and terrains of different geodynamic origin, such as ophiolites, island arcs, and active margin units and was overlain by the Transbaikalian magmatic units, some of which developed in response to subduction of the oceanic crust of the Paleo-Pacific Ocean (Yakubchuk, 2004; Buslov et al., 2004a; Windley et al., 2007). The eastern part of the Central Asian Orogenic Belt, formed during its collision with the Siberian craton, links the accretionary wedges of Central Mongolia and Circum-Pacific belts, the latter comprising accretionary complexes of Russian Far East and Japan (Parfenov et al., 1995; Badarch et al., 2002; Li, 2006; Dobretsov and Buslov, 2007; Fig. 1).

Fragments of paleooceanic islands and/or seamounts of the Paleo-Asian and Paleo-Pacific Oceans have been found in accretionary complexes of Transbaikalia (e.g., Gordienko et al., 2007), Altai-Sayan (e.g., Buslov et al., 2001; Dobretsov et al., 2004; Safonova et al., 2004),

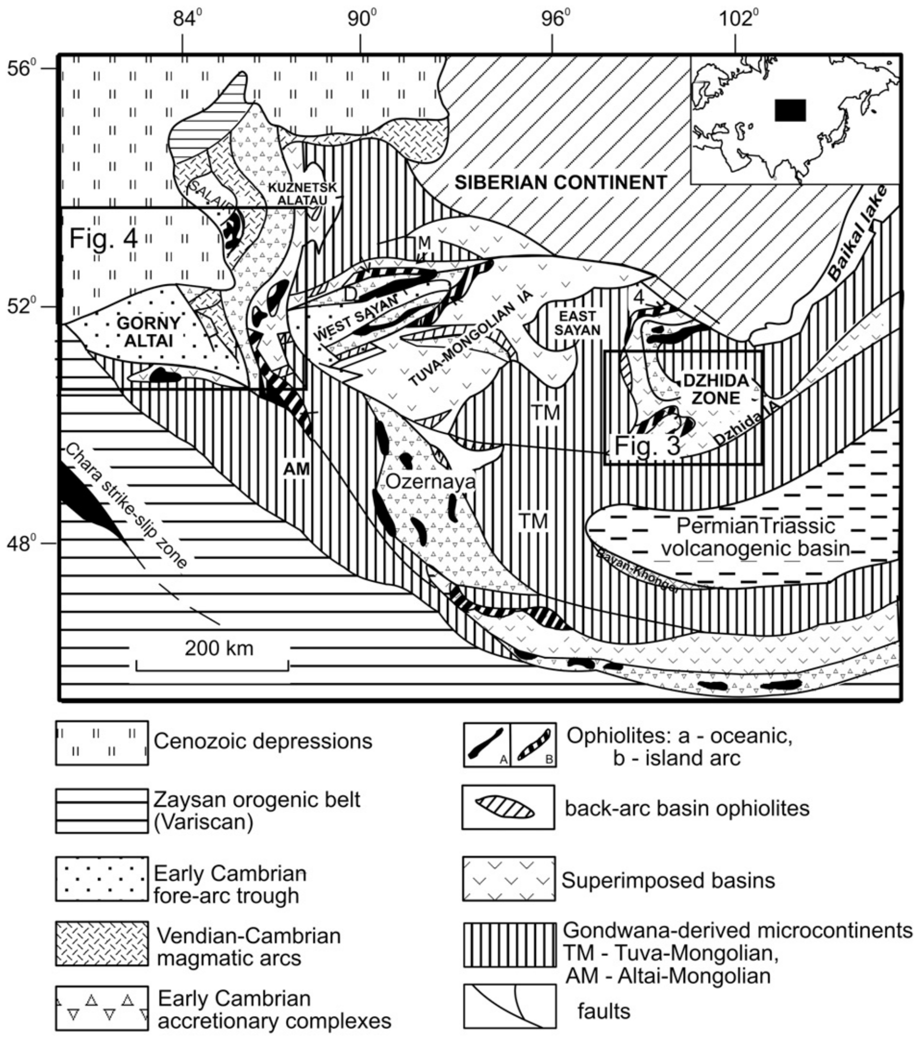

Fig. 2. Early Paleozoic accretion belts and Gondwana-derived Precambrian microcontinents of Altai-Sayan at the southern margin of the Siberian continent (modified from Buslov et al., 2001). IA—island arcs.

Russian Far East (e.g., Khanchuk et al., 1989b; Golozubov et al., 1992; Kojima et al., 2000) and Southwest Japan (e.g., Isozaki et al., 1990; Sano et al., 2000; Koizumi and Ishiwatari, 2006) (Figs. 2–5).

The present paper reviews localities of intraplate basalts of the Paleo-Asian and Paleo-Pacific Oceans, which occur as fragments of former oceanic islands, seamounts and plateaus in accretionary complexes of Altai-Sayan, Russian Far East and Southwest Japan and their related mineral deposits. Special emphasis is given to their relationships with associated OPS rocks, major and trace element chemistry and criteria for their identification in structurally complicated orogenic belts.

2. Geology and tectonics of OPS units and intraplate basalts

2.1. Paleo-Asian Ocean (Late Neoproterozoic to Carboniferous)

In the Paleo-Asian Ocean, paleo-islands were formed as a result of intraplate magmatism in a period from the Late Neoproterozoic to the Early Carboniferous. The paleo-islands were accreted to the ocean bounding island arcs and active margins of the Siberian continent and Gondwana-derived microcontinents as a result of oceanic subduction, which were later involved in processes of accretion and collision (Buslov et al., 2001). Their fragments occur within the Dzhida (1), Kurai (2), Katun (3), Charysh-Terekta (4) and Char (5) accretionary complexes (ACs) of Altai-Sayan (Southwest Siberia) and East Kazakhstan (Fig. 2; Table 1; the "Char" belt – named after River Char – is the same as that formerly mentioned "Chara" belt, e.g., Safonova et al., 2004, which is no longer considered correct). All localities of intraplate lavas are characterized by their association with OPS members: shallow-marine carbonate cap/reef limestone, hemipelagic carbonate-terrigenous–

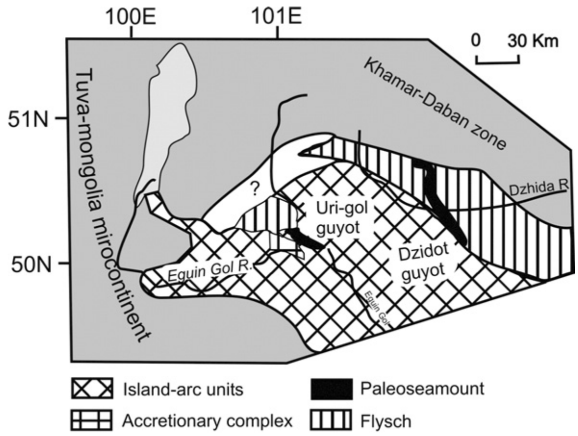

Fig. 3. Main units of the Dzhida orogenic zone (Gordienko et al., 2007).

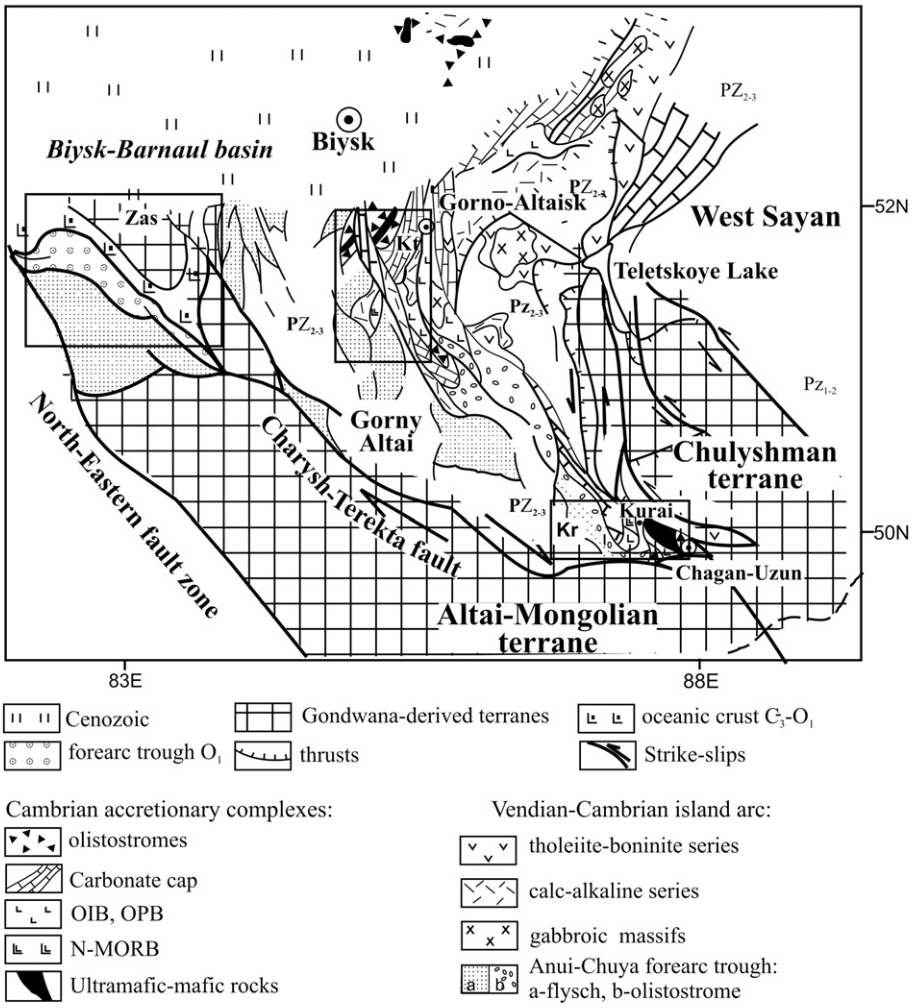

Fig. 4. Regional geology of Gorny Altai and location of Kurai (Kr), Katun (Kt) and Zasur'ya (Zas) accretionary complexes (modified from Buslov et al., 2001).

siliceous slope facies, pelagic bedded and/or radiolarian chert. These will be described in turn.

(1) *The Dzhida AC* is located between the Tuva–Mongolian microcontinent and Khamar–Daban zone of the Siberian Craton (Fig. 2). It comprises island-arc units and an accretionary complex hosting Urgol and Dzhidot paleoseamounts (Fig. 3). The OIB-type basalts of the Urgol paleoseamount are overlain by hemipelagic fine carbonate breccia (slope facies) and shallow-marine limestone and dolomite ("carbonate cap") containing an Early Cambrian algal assemblage (Gordienko et al., 2007). The Dzhidot seamount consists of tholeiitic and subalkaline basalts possessing OIB geochemical features, which are associated with oolitic limestone ("carbonate cap") and siliceous mudstone, pelitic siltstone and volcanic clastics (slope facies). The age of the unit is constrained by algal and miospore assemblages between the Ordovician–Silurian and latest Devonian (Gordienko et al., 2007; Ruzhentsev et al., 2005). The Urgol seamount was accreted to the Early Cambrian Dzhida island arc in the Early Ordovician and the Dzhidot paleoseamount was accreted to the Khamar–Daban active margin of the Siberian continent in the Late Devonian. Later both paleoseamounts were incorporated into the foldbelt during the closure of the central part of the Paleo-Asian Ocean in Carboniferous–Permian time (Gordienko et al., 2007).

(2 and 3) In Gorny Altai, SW Siberia, Late Neoproterozoic–Early Cambrian oceanic basalts are common within the accretionary prism of the Kuznetsk–Altai island arc, which includes the Kurai and Katun ACs (Fig. 4) (e.g., Dobretsov et al., 2004; Buslov et al., 2001; Safonova et al., 2004; Uchio et al., 2004). The intraplate basalts of Late Neoproterozoic and Early Cambrian age will be referred to as Kurai and Katun paleoseamounts, respectively, which were incorporated into the Kurai and Katun ACs during their Late Cambrian amalgamation with the Kuznetsk-Altai island arc and subsequent closure of the western part of the PAO.

(2) The Kurai paleoseamount of *the Kurai AC* consists of basaltic pillow lavas and dikes and associated sedimentary rocks, alternating with tectonic sheets of olistostromes, peridotites and serpentinitic mélange hosting high-pressure rocks (Buslov et al., 2001; Dobretsov et al., 2004). The seamount basalts are in direct contact with oceanic sediments like reef limestone with ooides and stromatolites (carbonate cap) and hemipelagic siliceous mudstone, clastic limestone and other terrigeneous slope facies sediments, possessing characteristic features of their formation of oceanic islands slopes: synsedimentary folding and brecciation (Safonova et al., 2008). The Late Neoproterozoic age of the basalts was estimated based on the 598 ± 25 Ma Pb–Pb isochron age of their associated limestone of the Baratal Formation (Uchio et al., 2004) (Fig. 5).

(3) The Katun paleoseamount is hosted by *the Katun AC*, which is situated north of the Kurai AC (Fig. 4). It comprises tholeiitic and alkaline basalts, clastic limestone, siliceous mudstone and dolomite of slope facies and carbonate cap bedded limestone

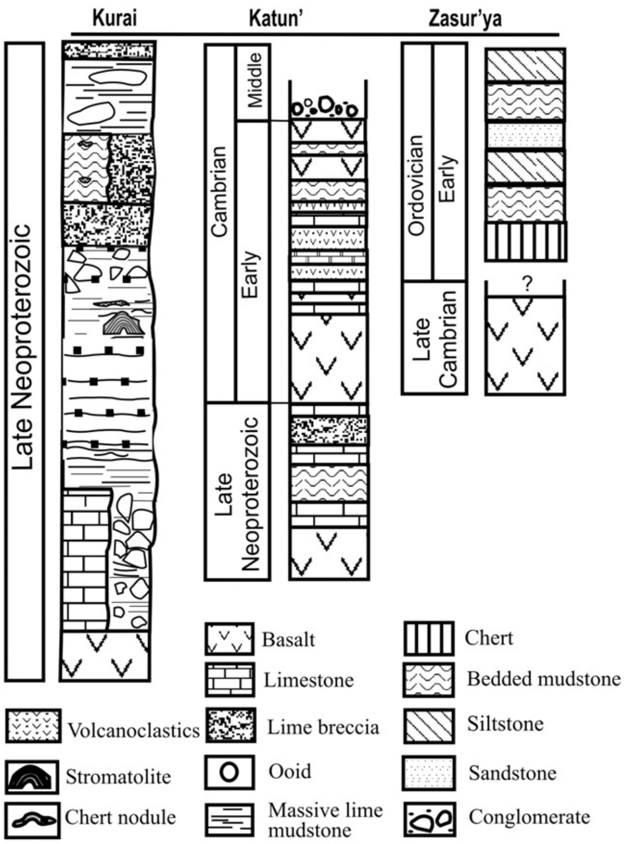

Fig. 5. Oceanic plate stratigraphy columns reconstructed in Altai-Sayan accretionary complexes – Kurai, Katun and Zasur'ya – compiled using materials from Uchio et al., 2004; Terleev, 1991; Sennikov et al., 2003, respectively.

and dolomite. It was suggested (Buslov et al., 2001; Dobretsov et al., 2004; Safonova et al., 2004) that these units represent fragments of a single unit of carbonate, siliceous, terrigenous and ocean island volcanic rocks formed in an oceanic island setting (Fig. 5). Carbonate and siliceous varieties have a breccia-like texture and show traces of submarine slumping. Fragments of the Katun paleoseamount occur in association with olistostromes similar to those of the Kurai AC (Buslov et al., 2001). Evidence for the Early Cambrian age of the Katun paleoseamount comes from the occurrence of abundant remnants of microphytoliths and calcareous algae in carbonates and sponge spicules in siliceous shale (Cheposh Formation; Terleev, 1991). Moreover, the whole structure of the Katun AC is stratigraphically overlain by basal conglomerates and then Middle Cambrian island-arc units (Repina and Romanenko, 1964).

(4) The Early Ordovician intraplate basalts of *the Zasur'ia AC* or Series are situated within the Charysh-Terekta strike-slip zone, which separates the units of the Siberian and Altai-Mongolian continents (Buslov et al., 2001; Fig. 4). The Zasur'ia Series consists of pillow lavas and pyroxene-plagioclase porphyritic basalts (and their volcaniclastic derivatives, sills and dikes) associated with multi-colored sandstones and cherts (Buslov et al., 2001; Sennikov et al., 2003; Fig. 5). The cherts are characterized by brecciation and Z-shape folding textural features suggesting their formation on the slopes of an oceanic island. The Zasur'ia Series consists of three formations with hidden contacts; probably because the rocks were displaced in respect to each other along strike-slip faults (Buslov et al., 2004b). The Early Ordovician age of the OPS units of the Zasur'ia Series is constrained by the occurrence of Late Cambrian–Early Ordovician pelagic conodonts and radiolarians with siliceous skeletons and sponge spicules (Iwata et al., 1997b; Sennikov et al., 2003). The proposed oceanic islands of the Zarus'ia formation were probably accreted to the active margin of the Gondwana-derived Altai-Mongolian microcontinent before its Late Devonian collision with the Siberian continent (Buslov et al., 2004a).

(5) The Late Devonian–Early Carboniferous OIB-type intraplate basalts of the Char strike-slip zone including *the Char AC* (Fig. 2) also occur as tectonic sheets and blocks in mélange, where they are associated with massive limestone, siliceous slope facies and pelagic chert. The cherts (Karabaev and Terentjev Formations) contain Late Devonian radiolarians, whereas the limestone intercalated with siliceous sediments (Verochar Formations)

Table 1
Intraplate basalts of the Paleo-Asian and Paleo-Pacific Oceans and their hosting accretionary complexes (ACs): age, location, geodynamic stage.

Age of intraplate magmatism	Hosting oceanic plate	Intraplate basalts and accretionary complexes	Geodynamic stage of incorporation of oceanic islands and seamounts into an AC
I. Paleo-Asian Ocean (640–340 Ma)			
Late Neoproterozoic–Early Cambrian	Paleo-Asian Ocean (maximal opening)	*Dzhidot and Urgol paleoseamounts*, Dzhida AC	Early Ordovician–Late Devonian accretion of seamounts to the Dzhida IA and active margin of the Siberian continent, respectively; (Gordienko et al., 2007)
Late Neoproterozoic, 600 ± 25 Ma;	Paleo-Asian Ocean	*Kurai paleoseamount*, Kurai AC	Early–Middle Cambrian accretion of seamounts to the Kuznetsk-Altai island arc at the margin of the Siberian continent
Early Cambrian;		*Katun paleoseamount*, Katun' AC	(Buslov et al., 2001; Dobretsov et al., 2004; Safonova et al., 2004)
Late Cambrian–Early Ordovician;		*Fragments of seamounts* in the Zasur'ia Series; Charysh-Terekta AC	Late Ordovician–Early Devonian accretion of seamounts to the active margin of the Altai-Mongolian microcontinent (Buslov et al., 2001; Safonova et al., 2004)
Late Devonian–Early Carboniferous;	Paleo-Asian Ocean (closure)	*Fragments of seamounts* in the Karabaev and Verochar Fms.; Chara AC	Late Carboniferous–Early Permian accretion of seamounts to the active margin of Siberian continent (Buslov et al., 2001; Safonova et al., 2004)
II. Paleo-Pacific Ocean (320–140 Ma)			
Carboniferous	Farallon Plate	*Akiyoshi-Sawadani seamount* chain, FP Akiyoshi and Khabarovsk (?) ACs	Early Permian subduction of the FP beneath the Yangtze Block and accretion of the seamount chain to the southern margin of the Yangtze block (Kanmera et al., 1990; Maruyama et al., 1997);
Permian	Farallon Plate; Izanagi Plate	*Maizuru plateau* (FP); Maizuru AC	Early Triassic accretion of the seamounts and plateau to the amalgamated Yangtze and Sino-Korean blocks (Maruyama et al., 1997)
		Akasaka-Kuzuu seamount chain Mino-Tamba and Samarka ACs	Early–Middle Jurassic orthogonal subduction of the Izanagi Plate beneath amalgamated Asia; Middle Jurassic accretion of seamounts to East Asia (Isozaki, 1997; Maruyama et al., 1997);
Late Jurassic	Izanagi Plate	*Mikabu plateau and seamounts*; Southern Chichibu and Taukha ACs	Early Cretaceous oblique subduction of the Izanagi Plate beneath East Asia and accretion of the plateau (Maruyama et al., 1997)

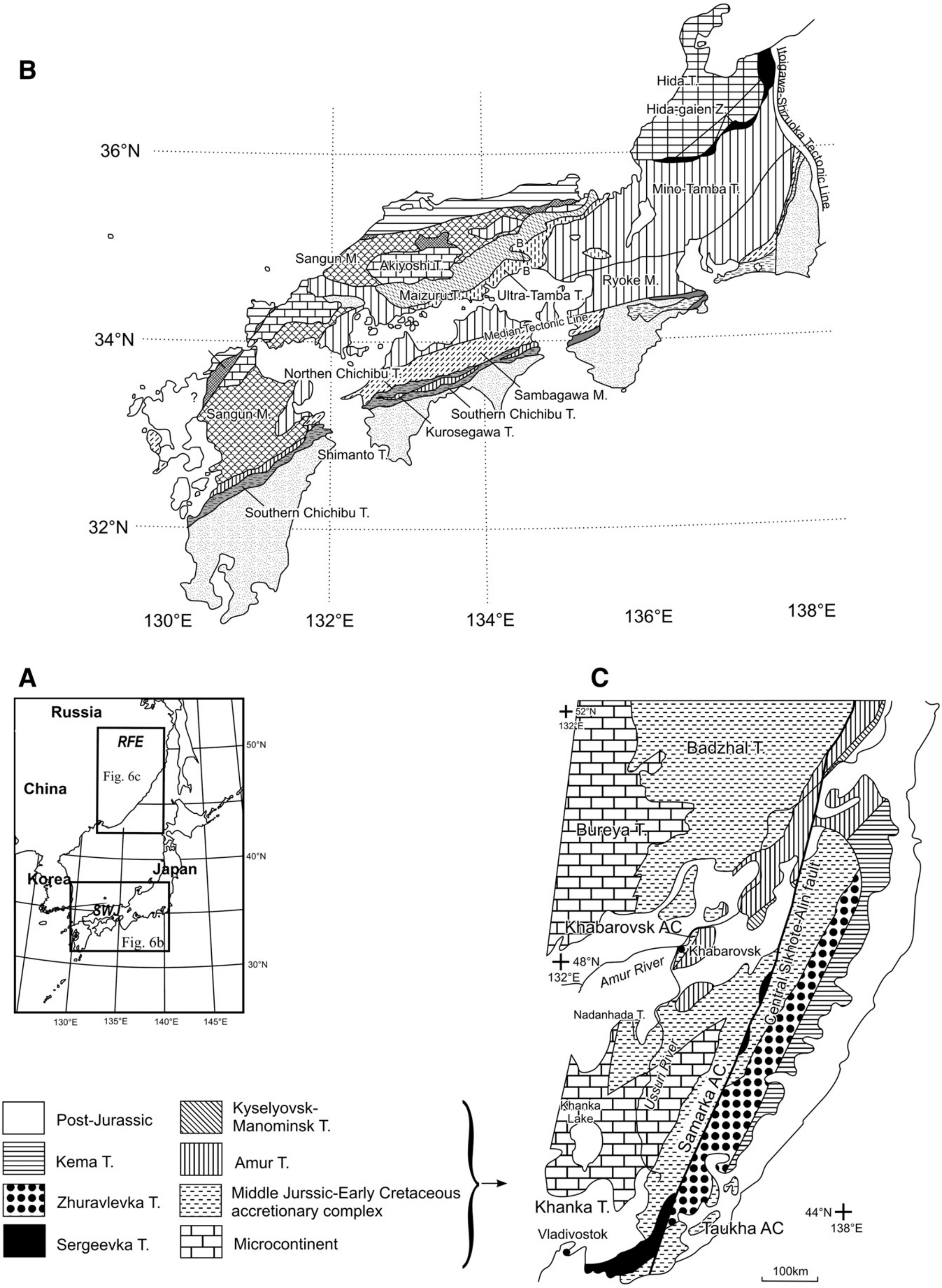

Fig. 6. Geographic and tectonic framework of Russian Far East (RFE) and Southwest Japan (SWJ). A—index map for RFE and Southwest Japan. B—Tectonic map of Southwest Japan. C—Tectonic map of southern RFE. T—terrane. Legend—for C.

hosts Early Carboniferous radiolarians (Iwata et al., 1997a; Sennikov et al., 2003). This agrees well with the general model of OPS implying that pelagic sediments may be both younger and older than the shallow-water seamount top carbonates (Isozaki et al., 1990). All tectonic sheets and blocks have been displaced along the strike-slip fault by tens and possibly hundreds of kilometers, which made the picturing of a more or less reliable lithologo-stratigraphic column impossible. The Char oceanic island basalts were probably formed in the NE branch of the Paleo-Asian Ocean and accreted to the active margin of the Siberian continent during its Late Carboniferous collision with the Kazakhstan continent and subsequent ocean closure (Buslov et al., 2004a; Safonova et al., 2004).

2.2. Paleo-Pacific Ocean (320–140 Ma)

In the western Paleo-Pacific Ocean or Panthalassa (Scotese and McKerrow, 1990; Maruyama et al., 1997), oceanic islands and plateaus formed from the Carboniferous until the Late Jurassic and were incorporated into accretionary units of the 6000 km long Circum-Pacific accretionary megabelt (Fig. 1). Subduction of the Farallon, Izanagi and Pacific plates continued from the Permian until the Early Cretaceous (Isozaki, 1997; Maruyama et al., 1997) and resulted in accretion of Paleo-Pacific seamounts and plateaus to the East Asian continental margin and the formation of accretionary complexes of Russian Far East and Southwest Japan. The Carboniferous Akiyoshi-Sawadani seamount chain was accreted to the Yangtze Block during the Early Permian subduction of the Farallon Plate and is presently hosted by the Akiyoshi AC (Isozaki et al., 1990; Maruyama et al., 1997). In the Early–Middle Jurassic, the Permian Akasaka-Kuzuu seamount chain was accreted to the Yangtze continental margin due to the subduction of the Izanagi plate (Mino-Tamba AC). In the Early Cretaceous, the Late Triassic Mikabu plateau was accreted to the East Asian active margin and incorporated into the Chichibu AC (Maruyama et al., 1997). At ca. 15 Ma, Japan split off East Asia (Khanchuk and Kemkin, 2003) resulting in the separation of once unified OPS units and accretionary complexes, which presently outcrop on both shores of the Sea of Japan: Russian Far East and Southwest Japan. In Russian Far East, fragments of oceanic islands and plateaus are hosted by Khabarovsk, Samarka and Taukha ACs, which are regarded as probable counterparts of the Akiyoshi (?), Mino-Tamba and Chichibu ACs of Southwest Japan, respectively (e.g., Matsuoka and Yao, 1990; Golozubov et al., 1992; Isozaki, 1997; Kojima et al., 2000, Suzuki et al., 2005) (Table 1; Fig. 6).

(6) *The Akiyoshi AC* and its supposed Russian Far East continuation the Khabarovsk AC (Fig. 6B, C) host the fragments of Carboniferous intraplate basalts, which are Akiyoshi-Sawadani seamounts according to the paleogeographic reconstructions of Maruyama et al. (1997). The Akiyoshi and Maizuru ACs are regarded as parts of a single two-phase accretionary belt following the same authors. According to Isozaki et al. (1990) the Akiyoshi terrane is dominated by limestone units and the Maizuru terrane is dominated by ophiolitic units. The Akiyoshi AC includes both continental (terrigenous clastics) and oceanic (radiolarian chert, basalt and reef limestone) units. The Middle Carboniferous–Permian age given to the limestone and chert was determined by microfossils: fusulinids, conodonts and radiolarians (Isozaki, 1997). The base of the limestone unit (Visean age) is directly underlain by pillow lavas of OIB-type basalts (Sano et al., 2000). Isozaki (1997) regarded the bedded chert and limestone as pelagic and shallow-marine OPS complexes, respectively, which once occurred upon a basaltic seamount/oceanic island (Fig. 7). In general, the Akiyoshi terrane, which consists of a large reef limestone sequence with underlying alkaline basalts, is an excellent example of a collapsed ancient intraplate oceanic island/seamount (Sano and Kanmera, 1991; Isozaki, 1997).

The schematic age-lithostratigraphic diagram (Fig. 7) shows that *the Khabarovsk AC* comprises two OPS sedimentary units of different ages

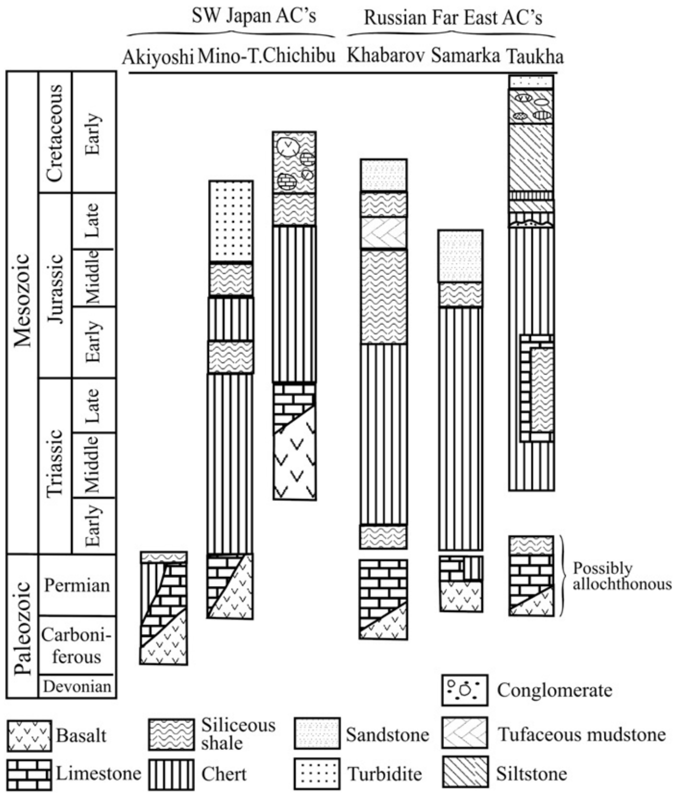

Fig. 7. Oceanic plate stratigraphy columns reconstructed in accretionary complexes of Russian Far East and Southwest Japan based on the data of Isozaki et al., 1990; Isozaki, 1997; Matsuoka and Yao, 1990; Mizutani, Kojima, 1992; Suzuki et al., 2005; Golozubov et al., 1992; Wakita, Metcalfe, 2005.

(based on paleontological data): Carboniferous–Permian and Triassic–Early Jurassic, each consisting of pelagic chert, shallow-water limestone and basalt (Noda, 1956; Shevelev, 1987; Mizutani and Kojima, 1992; Bragin, 1992; Suzuki et al., 2005). The older unit can be correlated with the Akiyoshi AC because of their close ages, similar proportions of OPS units and OIB-type geochemistry of associated basalts (Table 3; Figs. 7–11). The younger OPS unit can be correlated with the Mino-Tamba AC, because it consists of Triassic ribbon chert and reef limestone overlain by Jurassic siliceous mudstone (Suzuki et al., 2005).

(7) The Jurassic *Mino-Tamba AC* occupies a large part of SW Japan (Fig. 6B) and is thought to extend north to Sikhote-Alin and northeast to China (Kojima et al., 2000). It has been studied extensively because it includes the well-known Inuyama area with a complete OPS succession (e.g., Kondo and Adachi, 1975; Sano and Kanmera, 1991; Sano and Kojima, 2000; Wakita, 2000). The Mino-Tamba AC is composed of accreted oceanic material such as Carboniferous–Permian basalts and limestone and Permian–Jurassic chert. The Mino-Tamba OPS units are similar to those of *the Samarka AC* or terrane in southern Sikhote-Alin of RFE (Fig. 6C) in lithology, age, geological structure and faunal assemblage: Kojima et al. (2000) argued that the Samarka terrane is the northern extension of the Mino-Tamba terrane by correlating both sedimentary and magmatic sequences. The oceanic rocks of both terranes comprise two lithologically different sedimentary assemblages (Sano and Kojima, 2000; Kojima et al., 2000; Nakae, 2000; Ishiwatari and Nakae, 2001). The first is a shallow-marine assemblage chiefly of Permian bioclastic limestone. The second is a pelagic assemblage dominated by Lower Permian to Upper Jurassic bedded radiolarian cherts and related siliceous rocks. Both the Permian carbonates and bedded cherts overlie the basaltic succession (Fig. 7). Sano and Kojima (2000) considered that the Permian carbonates accumulated to form a buildup at the top of a basaltic oceanic rise, presumably a seamount.

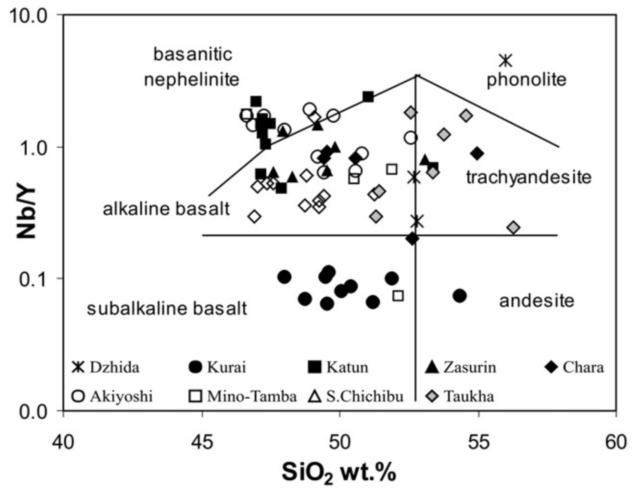

Fig. 8. Nb/Y versus SiO_2 classification diagram (Winchester and Floyd, 1977).

According to the reconstructions by Maruyama et al. (1997) the Permian basalts of the Mino-Tamba AC can be regarded as fragments of the former Paleo-Pacific Ocean Akasaka-Kuzuu seamount chain. Due to active tectonics and deformation which took place during Cretaceous times along the East Asia active margin (Isozaki et al., 1990; Maruyama et al., 1997) separate fragments of two seamount chains, Akiyoshi-Sawadani and Akasaka-Kuzuu, could have been juxtaposed in the Mino-Tamba AC. However, the question of possible tectonic juxtaposition of the Carboniferous and Permian basaltic units is still open and needs further research.

(8) The Chichibu AC of Jurassic–Early Cretaceous age is the third large accretionary belt of Southwest Japan, located south of the Mino-Tamba AC (Fig. 6B). In general, the Chichibu area consists of three terranes: northern Chichibu, Kurosegawa and southern Chichibu. The northern Chichibu is close to the Mino-Tamba AC and sometimes this structure is referred to as Mino-Tamba-Chichibu belt (Maruyama et al., 1997). *The Southern Chichibu AC* extends over 1000 km from the Kyushu Island to the Kanto Mountains and consists of the Togano and Sambosan terranes (or Sanbosan) characterized by different lithologies and age (Matsuoka and Yao, 1990; Isozaki et al., 1990; Tatsumi et al., 2000). The Southern Chichibu AC (Sambosan) hosts voluminous OIB-type basalts of Permian to Triassic age and chert-dominated OPS of Triassic–Jurassic age (e.g., Matsuoka, 1992; Onoue et al., 2004). Within the Sambosan area the OIB-type basalts are exposed as blocks within volcanogenic clastic rocks and brecciated fragments of pillowed basalts interbedded with Middle Triassic chert (Fig. 7). The blocks of basalts are up to several tens of meters in size and consist mainly of basaltic pillows cemented by carbonate matrix and subordinate lavas and hyaloclastic rocks (Onoue et al., 2004). Based on the suggested Triassic age of basalts and the reconstructions made by Maruyama et al. (1997) the OIB's hosted by the Chichibu AC may have been derived from the Mikabu plateau.

A possible Russian analogue of the Southern Chichibu is Taukha AC (Golozubov et al., 1992; Kojima et al., 2000), which is located at the southern end of the Sikhote-Alin' Mountains (Fig. 6C). Similarly, *the Taukha AC* or terrane consists of radiolarian chert, siliceous mudstone, sandstone, Z-folded clastic rocks, intraplate basalts or paleoguyots (Khanchuk et al., 1989a; Golozubov et al., 1992; Fig. 7). Estimates on the age of the basalts vary. The “carbonate cap” limestones directly are underlain by OIB-type basalts containing Middle and Late Triassic conodonts, mollusks and corals. Their associated chert assemblages contain radiolarians of Middle Triassic to Late Jurassic (Dal'negorskiy area) and Jurassic–Early Cretaceous (Kavalerovo area) ages (e.g., Khanchuk et al., 1989a; Volokhin et al., 1990; Bragin, 1991; Golozubov et al., 1992).

3. Petrography and geochemistry of intraplate basalts

3.1. Petrography

The volcanic rocks display diverse petrographic textures, ranging from fine- to medium-grained porphyritic to aphyric, although porphyric lavas are dominant. Amygdaloidal textures are also typical with amygdales usually filled by calcite and chlorite. The phenocrysts in the porphyritic varieties are plagioclase, clinopyroxene and olivine. Groundmass is variolitic, microlitic or hyalopilitic. Opaque minerals, principally magnetite, are present as accessory phases.

In general, the Late Neoproterozoic and Early Paleozoic basalts have undergone stronger post-magmatic alteration than the Late Paleozoic and Mesozoic basalts. However, the Char basalts of Late Devonian–Early Carboniferous age have also been strongly altered because they occur within a strike-slip deformation zone (Buslov et al., 2001; Safonova et al., 2004). Olivine, pyroxene and volcanic glass are partly or completely replaced by chlorite and epidote, and plagioclase by albite. Although most basalts have been metamorphosed in the greenschist facies and contain abundant alteration minerals such as epidote, chlorite and albite, they display well-preserved original igneous textures (Table 2).

3.2. Geochemistry of intraplate basalts

The analytical data on the Dzhida, Kurai, Katun, Zasur'ya and Char ACs (Transbaikalia and Altai-Sayan) were obtained by XRF (major elements), INAA (REE) and ICP MS (REE plus Rb, Sr, Y, Zr, Nb, Ba, Th, Hf, etc.) (Safonova et al., 2004; Safonova, 2005; Gordienko et al., 2007; Safonova et al., 2008). All the original data on the Kurai, Katun, Zasur'ya and Char ACs are of good quality and well within international standards; the analytical errors on most REE and HFSE (high-field strength elements) are within 5 to 10% (Safonova, 2005). The data on the Akiyoshi, Mino-Tamba and Chichibu ACs of Japan (Sano et al., 2000; Tatsumi et al., 2000; Ichiyama and Ishiwatari, 2005; Koizumi and Ishiwatari, 2006; Ichiyama et al., 2006; Table 3) were obtained by XRF (major and transitional elements plus HFSE) and INAA (REE and HFSE). The error ranges of INAA are 3 to 6% for Cr, La, Ce, Sm and Eu, and 10–20% for Hf, Ta, Th, Ba, Yb and Lu (Ichiyama and Ishiwatari, 2005). The above cited papers presented no information on the XRF analytical errors and consequently the latter are not considered in this paper.

Due to the high degree of alteration, all major element data are recalculated on a volatile-free basis. Variable element mobility is a possibility for volcanic rocks that have undergone seafloor hydrothermal alteration, greenschist to amphibolite facies metamorphism, and tectonic deformation. Nevertheless, there is general agreement that rare-earth elements (REE), high-field strength elements (HFSE), and some transition metals are least sensitive to mobility (e.g., Winchester and Floyd, 1977; Ludden et al., 1982; Condie, 1994). Light REE are more sensitive to secondary processes compared to middle REE and heavy REE, however the mobility of REE takes place only at high water/rock ratio or during carbonatization (Humphris, 1984), which is not observed in our case. Besides, evidence for low mobility of HFSE, REE (except Eu) and, to a lesser degree, Th include the following: (1) there is no significant enrichment or depletion of groups of elements (e.g., light REE) in a given rock type over a range of L.O.I; (2) primitive mantle-normalized trace element diagrams of given suites of basalts associated in the field exhibit coherent patterns for Th, HFSE, and REE (Fig. 10); (3) Th/La_{pm} and Nb/La_{pm} do not correlate with the CIA (chemical index of alteration), Eu/Eu*, or loss on ignition (not shown here; Safonova, 2005; Safonova et al., 2008).

Thus, our trace and major element interpretation mainly focuses on relatively immobile elements (e.g., Zr, Ti, Nb and REE), which are likely to be less affected by alteration. Major and trace element data presented here represent a compilation of published data (Table 3 and references therein). Unfortunately, the trace element data on the Chichibu and Russian Far East ACs are very limited. For convenience, in

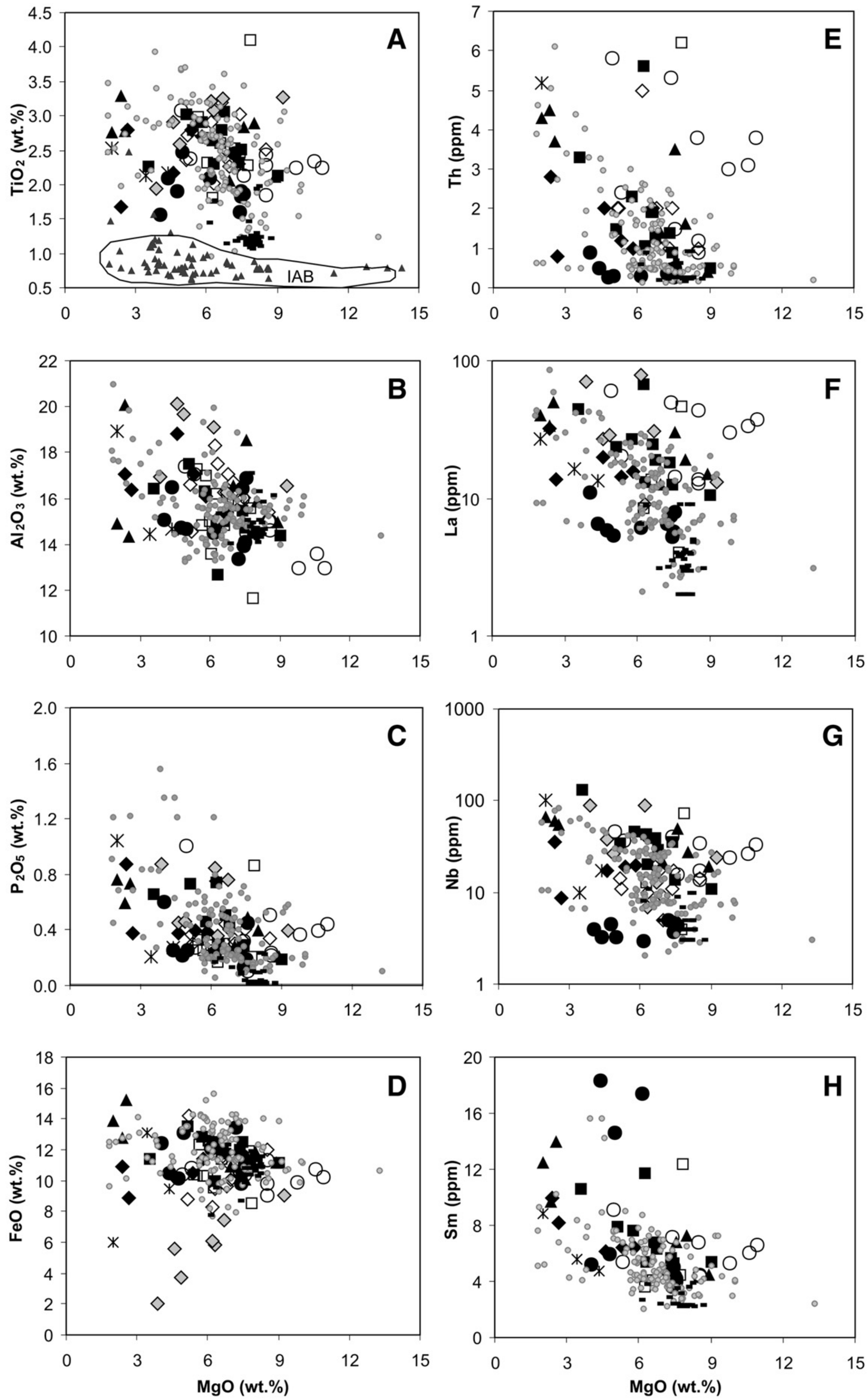

Fig. 9. Major and trace element data (ppm) versus MgO (wt.%) for basalt samples from the accretionary complexes of Russia and Japan. MgO data recalculated on a volatile-free basis. Small symbols: rectangles—Pacific MORB, triangles—IAB, circles—Emperor–Hawaii Chain (GEOROC database—www.georoc.mpch-mainz.gwdg.de/georoc). Other symbols as in Fig. 8.

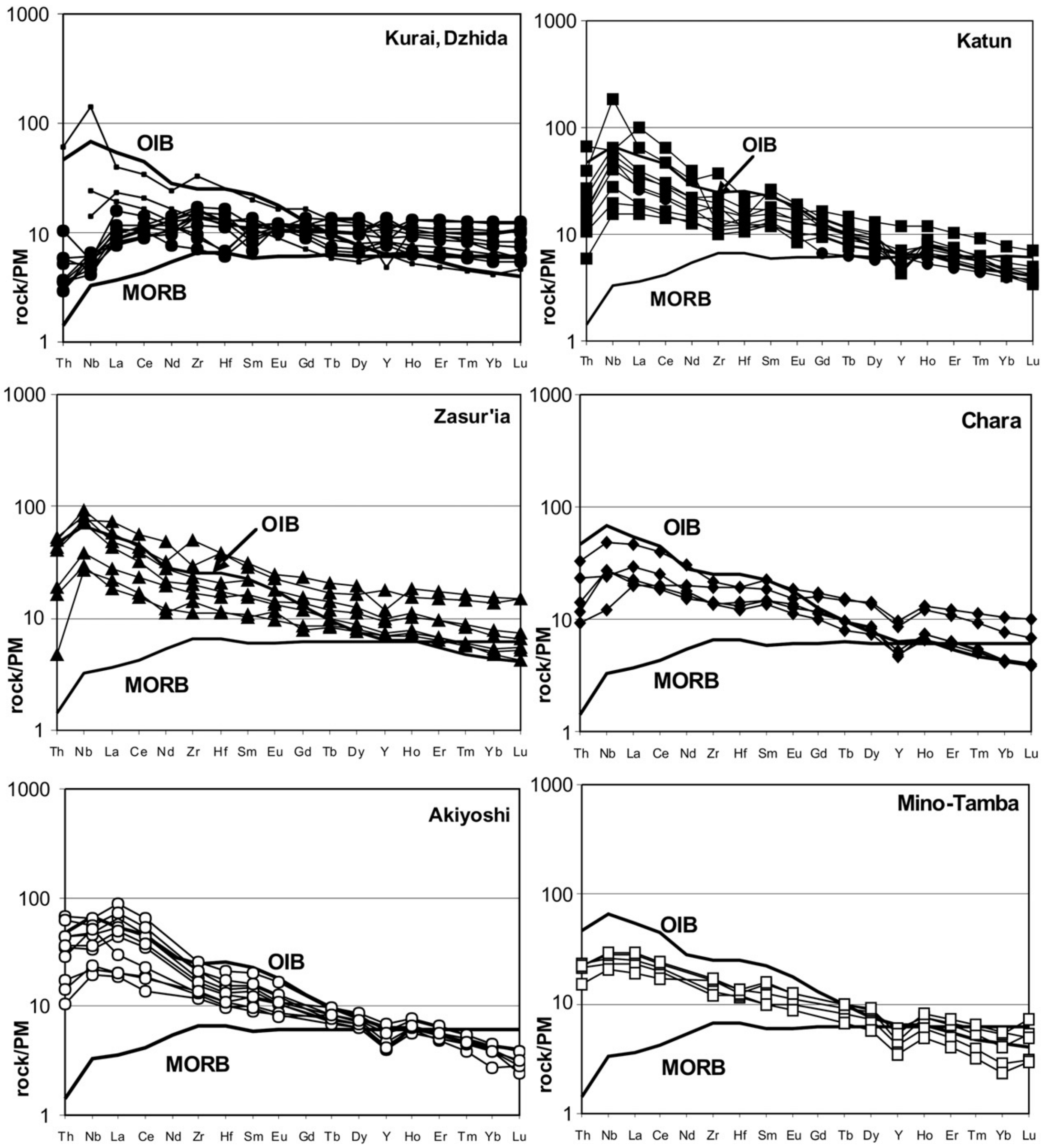

Fig. 10. Primitive mantle-normalized trace element diagrams for all basalt suites. OIB, MORB and normalization values are from Sun and McDonough (1989).

the succeeding diagrams, the dataset was divided into two groups based on their geographical location and relation to the Paleo-Asian and Paleo-Pacific Oceans, respectively: those recovered from accretionary complexes of Transbaikalia (Dzhida), Altai-Sayan (Kurai, Katun, Zasur'ia) and East Kazakhstan (Char) (stars and black symbols; Figs. 2–4), and those from accretionary complexes of Southwest Japan (Akiyoshi, Mino-Tamba, S. Chichibu; open symbols) and Russian Far East (Taukha) (gray rhombs; Fig. 6).

All samples are subalkaline to alkaline (trachy-) basalts in the total alkali-silica diagram (not shown here). The SiO_2 *vs.* Nb/Y classification diagram shows two groups of basalts: subalkaline and alkaline (Fig. 8). Alkaline basalts dominate and have been found in the OPS units of all accretionary complexes under consideration. The subalkaline basalts are more typical of the Kurai AC. In respect to the element relationships in the Al_2O_3–TiO_2+FeO^*–MgO system the majority of samples are tholeiitic and several Akioshi samples are calc-alkaline basalts (diagram not shown here).

3.2.1. Major element compositions

The main chemical characteristics of the different basalt suites are listed in Table 3. The major element data are generally similar with exception of Dzhida subalkaline basalts, which have lower Mg number (Mg#). Analyses of 74 representative samples selected from different publications (see footnote to Table 3) are illustrated in Fig. 9A–D. The principal major element characteristics of both groups have variable MgO (2 to 10 wt.%; the majority <8 wt.%) and Fe_2O_3(tot) (3 to 16 wt.%) contents, resulting in Mg# between 20 and 70. On average, the younger samples of Southwest Japan and Russian Far East have higher MgO and Al_2O_3 contents than the older basalts of Altai-Sayan and Kazakhstan ACs (Fig. 9; Table 3). TiO_2 concentrations vary between 1.5 and 4.1 wt.%,

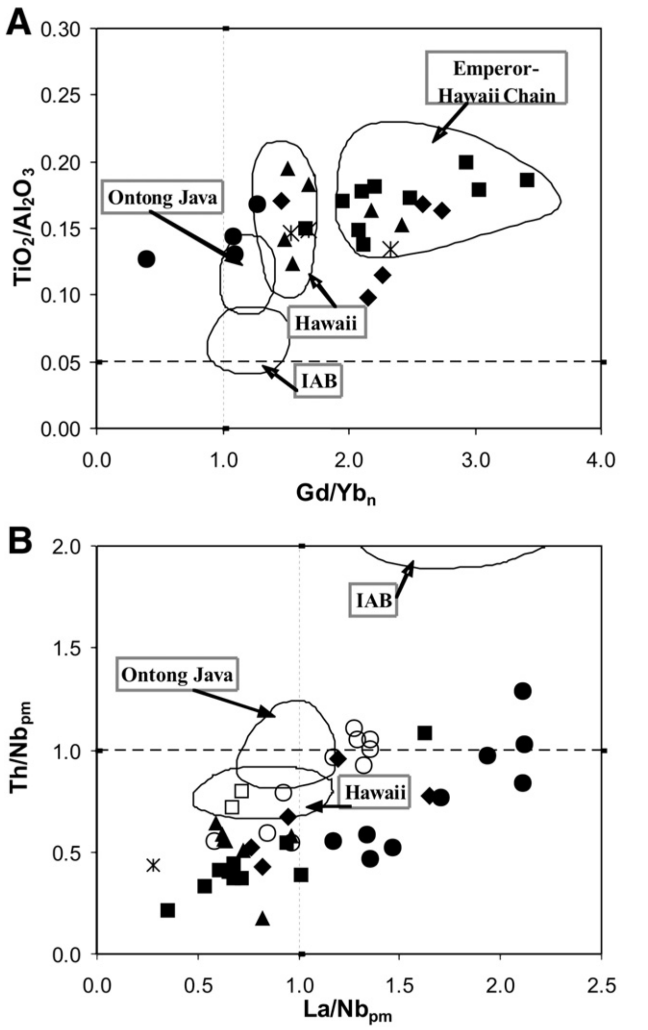

Fig. 11. TiO_2/Al_2O_3 vs. Gd/Yb$_n$ (A) and Th/Nb$_{pm}$ vs. La/Nb$_{pm}$ (B) for all basaltic units indicating low to medium degree of melting (A) and absence of crustal contamination (B) compared to other OIBs, oceanic plateau basalts and island-arc basalts (IAB). The outlined fields were compiled by the author using the GEOROC database (www.georoc.mpch-mainz.gwdg.de/georoc). Symbols as in Fig. 8.

and P_2O_5 is in the range 0.13 to 0.8 wt.%, with P_2O_5 showing enrichment with decreasing MgO in all groups except for the Mino-Tamba AC (Fig. 9D). In the TiO_2, Al_2O_3, Fe_2O_3 and P_2O_5 *vs.* MgO diagrams (Fig. 9A–D) data are scattered revealing no general elevation in TiO_2, Al_2O_3, Fe_2O_3(tot) and P_2O_5. Both TiO_2 and Fe_2O_3(tot) increase slightly with decreasing MgO, suggesting that magnetite or titanomagnetite were not major fractionating phases, except for the Taukha basalts which show a stronger positive correlation. SiO_2 spans 45 to 55 wt.% (average 48 wt.%); Al_2O_3 varies between 13 and 20 wt.% and generally increases with decreasing MgO suggesting simultaneous fractionation of clinopyroxene and plagioclase in the Katun, Akiyoshi and Taukha basalts (Fig. 9b; Table 3).

3.2.2. Trace element compositions

The basalt trace element characteristics are partly illustrated in Fig. 9E–H and shown in Table 3. Nickel and Cr concentrations are typically low, with averages around 75 and 179 ppm, respectively, consistent with the evolved nature of these samples indicated by the generally low Mg#. No samples display both high Ni and Cr, which is thought to be consistent with a primitive magma composition. The correlation between Ni, Cr and MgO in most rock groups is in support of the above suggestion, that both olivine and pyroxene fractionation has occurred.

Nb (2 to 130 ppm), Y (14 to 80 ppm) and Zr (55 to 600 ppm) all show weak to moderate increase with decreasing MgO as expected by fractionation of plagioclase, olivine and clinopyroxene (Fig. 9D). The majority of the samples have Zr/Nb ratios from 6 to 14, similar to ratios found in many OIB's (e.g., Emperor–Hawaii seamount chain, Regelous et al., 2003), although samples from the Kurai AC having significantly higher Zr/Nb ratios of about 31, similar to some ocean plateau basalts (e.g., Ontong Java Plateau, Mahoney et al., 1993). Ti/Zr ratios are in the range of 69 to 93 (Table 3) implying different conditions of formation, controlled by either the composition of the source, the nature of partial melting, the extent of contamination and/or the extent of titanomagnetite fractionation.

The majority of basalts from all accretionary complexes are light-REE-enriched relative to chondrite (La/Sm$_n$ = 1.6 to 3.1), with almost no Eu anomalies (Eu/Eu* = 0.93 to 1.09). Eu/Eu* was calculated following the method of Taylor and McLennan (1985)—i.e., referenced to Sm and Gd. HREE (heavy REE) concentrations (Gd to Lu) are slightly higher in the Kurai basalts compared to other localities, however, the degree of HREE fractionation is higher in the latter (1.1 *vs.* 1.6–2.3; Table 3).

Fig. 10 displays trace and minor element data for selected samples normalized to primitive mantle (after McDonough and Sun, 1995). Alteration has modified the compositions of most of the samples analyzed and the concentrations of mobile trace elements in many of the samples cannot be considered as primary. Consequently, most large-ion lithophile elements (e.g., Ba, Rb and K) are here regarded as relatively mobile during post-magmatic alteration processes. In the Kurai basalts there are pronounced negative anomalies of Nb and Ti, which are distinctive features of oceanic plateau basalt. For example, the Ontong Java Plateau, the world's largest oceanic large igneous province, also shows low Nb and Ti abundances (Mahoney et al., 1993). The multi-component trace element diagrams of Katun, Zasur'ia, Char and Mino-Tamba basalts display prominent positive Nb anomalies with respect to La (Nb/La$_{pm}$ = 1.3 to 1.5), whereas patterns for Kurai, Akiyoshi and Taukha basalts weakly peak at La and have smoother convex-up patterns through La, Nb and Th (Nb/La$_{pm}$ = 0.7 to 0.9). In all samples, Th is depleted in respect to Nb and La (Th/La$_{pm}$ = 0.5 to 0.8; Nb/Th$_{pm}$ = 1.1 to 2.6; Table 3; Fig. 11B). Similar trace element patterns have been documented for many Phanerozoic

Table 2
Petrographic characteristics of samples.

Location (AC)	Rock type	Rock texture	Phenocrysts phasea	Groundmass	Reference
Dzhida	Basalt	Porphyritic	pl, cpx, ol	Variolitic	Gordienko et al. (2007)
Kurai	Basalt,	Porphyritic,	cpx, pl	Hyalopilitic	Safonova et al. (2008)
	Basalt	Aphyric,	–	–	
	Dolerite	Ophitic	pl, cpx	–	
Katun	Basalt	Aphyric,	–	–	Safonova et al., 2004; Safonova, 2005
	Dolerite	microporphyric	pl, cpx	Hyalopilitic	
	Andesitic basalt		pl, cpx	–	
Zasur'ia	Gabbro	Poikilophitic,	–	–	
	Dolerite	Ophitic,	–	–	
	Basalt	Porphyric	cpx, pl	Microlitic	
Chara	Basalt	Porphyritic,	pl, cpx	Intersertal	
	Basalt	Aphyric,	–	–	
	Dolerite	Ophitic,	pl, cpx	–	
	Andesitic basalt	Microporphyric	pl	Microlitic	
Mino-Tamba	Basalt	Porphyritic,	pl,cpx,ol	Intersertal	Koizumi and Ishiwatari (2006)
	Basalt	Aphyric,	–	–	
	Dolerite	Ophitic	pl, cpx	–	
S. Chichibu	Basalt	Porphyritic, aphyric	pl, ol, cpx –	Microlitic –	Onoue et al. (2004)
Taukha	Basalt	Porphyritic	ol, cpx	Hyalopilitic	Khanchuk et al. (1989a)

Abbreviations are as follows: pl = plagioclase, cpx = clinopyroxene, ol = olivine.

Table 3
Mean values of selected element abundances and ratios from the intraplate basalts of accretionary complexes in Russia and Japan.

Accretionary complex	1	2	3	4	5	6	7	8	9
	Dzhida	Kurai	Katun	Zasur'ia	Chara	Akiyoshi	Mino-Tamba	Chichibu	Taukha
	N = 3[a]	N = 15	N = 14	N = 9	N = 8	N = 17	N = 20	N = 20	N = 8
SiO_2	51.8	49.1	46.5	47.5	47.6	47.2	50.3	48.1	48.4
TiO_2	2.19	1.78	2.44	2.85	1.97	2.54	2.48	2.45	2.65
Al_2O_3	15.4	14.4	14.6	15.8	16.1	15.1	15.6	16.6	16.1
Mg#	32	51	50	42	48	58	54	54	41
Zr/Nb	9.2	31.6	6.3	6.5	8.3	7.3	14.5	12.0	12.6
La/Sm_n^b	1.8	1.6	1.9	2.1	2.1	3.1	2.3		
Gd/Yb_n	1.9	1.2	2.3	1.7	2.3	2.4	2.0		
Nb/La_{pm}	3.6	0.7	1.5	1.3	1.5	0.9	1.5		1.0
Th/La_{pm}	1.6	0.5	0.6	0.8	0.8	0.8	0.8		
Nb/Th_{pm}	2.3	1.4	2.6	2.0	2.0	1.2	2.4	1.0	
Al_2O_3/TiO_2	7.0	8.5	6.0	5.8	8.5	6.2	7.5	7.3	6.2
Eu/Eu*	0.94	1.07	0.93	1.09	0.96	0.97	1.01		
Ti/Zr	68.7	85.6	89.2	69.4	79.5	74.0	92.7	93.5	78.1

Data sources: 1—Gordienko et al. (2007); 2–5—Safonova, 2005, Safonova et al. (2004, 2008); 6—Sano et al. (2000); 7—Ichiyama et al. (2006), Koizumi, Ishiwatari (2006), Sano et al. (2000); 8—Tatsumi et al. (2000); 9—Khanchuk et al. (1989a).
[a] *N*—number of samples.
[b] *n* and *pm* denote normalization to chondrite and primitive mantle, respectively (McDonough and Sun, 1995). Mg# is calculated as [100*(MgO/FeO + MgO)] assuming Fe_2O_3/FeO of 0.15.

transitional to alkaline ocean island basalts (e.g., Chen et al., 1991; Weaver, 1991; Regelous et al., 2003).

In the TiO_2/Al_2O_3 *vs.* Gd/Yb_n diagram (Fig. 11A) all data plot in the OIB field forming a wide trend of TiO_2/Al_2O_3 ratios. OIB-type basalts are characterized by higher Gd/Yb_n and TiO_2/Al_2O_3 compared to MORB and IAB, respectively. All samples show Ti enrichment and medium to strong HREE fractionation, which is likely to be a garnet signature of mantle melting. Ratios of Gd/Yb_n decrease from 3.5 to 1 thus suggesting low to medium degrees of partial melting (Fig. 11A).

In the Th/Nb_{pm} *vs.* La/Nb_{pm} diagram (Fig. 11B) most samples plot below the line of $Th/Nb_{pm} = 1$, which conventionally separates crustally contaminated basalts from more primitive basalts (Polat et al., 1999), and form a continuous trend from OIB to oceanic plateau basalts. Crustal contamination is quite possible; however, numerous lines of geological evidence, provided by many geologists previously worked in that region, are consistent with an intra-oceanic setting for the basalt sequences (e.g., Buslov et al., 2001; Sennikov et al., 2003; Dobretsov et al., 2004; Safonova et al., 2004, 2008). Negative Nb anomalies in a part of basalts from the Kurai and Akiyoshi ACs could possibly reflect some crustal contamination (Fig. 10), however, the following is noted: (1) Nb/La_{pm} do not correlate with Th/La_{pm}; (2) Th contents are rather low (Table 3; Sano et al., 2000; Safonova et al., 2008); (3) geology-lithological relationships show that the basaltic units formed over the oceanic, not continental, lithosphere; (4) Nb and Th concentrations were obtained by XRF, which suggests rather high analytical errors, but this must be confirmed in future work.

The low Nb/La_{pm} values in some basalts possibly resulted not from contamination of tholeiitic liquids by continental crust during eruption (exogeneous contamination), but from recycling of lithosphere into the mantle during subduction of the oceanic slab (endogenous contamination) (Polat et al., 1999). The relatively low concentrations of Th (2 to 5 ppm that is typical of the average OIB of Sun and McDonough, 1989) also rule out crustal contamination (Sano et al., 2000; Tatsumi et al., 2000; Ichiyama and Ishiwatari, 2005; Gordienko et al., 2007; Safonova et al., 2008). Although, several samples of the Kurai, and Akiyoshi ACs plot above the $Th/Nb_{pm} = 1$ line (Fig. 11B) these basalts display much less Th enrichment, i.e., $Th/Nb_{pm} < La/Nb_{pm}$ or $Nb/La_{pm} > Th/La_{pm}$. (Fig. 10; Table 3). Most suprasubduction basalts (island-arc volcanics) are characterized by Th/Nb_{pm} ratio exceeding 2 (Fig. 11B).

Based on the data presented two geochemical types of Paleo-Asian Ocean and Paleo-Pacific Ocean intraplate basalts are recognized: (1) LREE (light REE), Nb and Ti enriched; and (2) transitional. In the trace element ratio binary diagrams two groups of basalts are undistinguishable and plot between the MORB and OIB lines/field (Fig. 11). The alkaline basalts are characterized by LREE-enriched patterns and positive Nb anomalies in the multi-component diagrams, whereas the transitional varieties have flatter REE regions of the patterns and display negative Nb anomalies in respect to La and, to a lesser degree, Th (Fig. 10). The basaltic units hosted by Kurai and Akiyoshi ACs include both rock types, whereas the other accretionary complexes incorporate only enriched varieties.

4. Discussion

In order to address problems of intraplate magmatism and oceanic plate stratigraphy of the Paleo-Asian and Paleo-Pacific Oceans, the author evaluates and discusses in turn questions of recognizing OPS units, geochemical variability of intraplate basalts, discrete or continuous character of intraplate magmatism, OPS-hosted mineral deposits in general, and criteria for identification of intraplate basalts specifically. All these would help us to understand better the history of two oceans, i.e., and to conclude about their mutually related or independent evolution.

4.1. Recognizing OPS units

Figs. 5 and 7 show many similar features in the Paleozoic (Paleo-Asian Ocean) and Mesozoic (Paleo-Pacific Ocean) OPS units hosted by accretionary complexes. Plume-related intraplate basalts, which are former parts of oceanic islands, seamounts and plateaus, occur at the base of all OPS units. These are overlain by bedded and massive limestone (carbonate cap) and other OPS elements: siliceous mudstone, calcareous mudstone, micritic limestone, lime-volcaniclastics (hemipelagic, slope facies) and bedded/ribbon/radiolarian chert (pelagic facies). However, the older the seamounts, the less preserved are pelagic chert facies. Bedded chert has been found in all Late Paleozoic and Mesozoic localities—Char, Akiyoshi, Khabarovsk, Tamba-Mino, Samarka, Chichibu, Tauka ACs (in order of increasing amount) and in lesser proportion in the Zasur'ia Series of Early Ordovician age (Isozaki et al., 1990; Golozubov et al., 1992; Sennikov et al., 2003). When compared it is evident that the oldest Akiyoshi AC of Southwest Japan is dominated by limestone relative to chert, whereas the younger Mino-Tamba and Southern Chichibu ACs are dominated by chert (Isozaki et al., 1990). In the Southern Chichibu AC the proportion of chert to limestone ranges from 3:1 to 20:1 (Onoue et al., 2004). The older Zasur'ia AC of Late

Cambrian–Early Ordovician age contain less chert than the younger Char AC of Late Devonian–Early Carboniferous age (Sennikov et al., 2003). No pelagic chert has been found in the Late Neoproterozoic Dzhida and Kurai AC and the Early Cambrian Katun' ACs, which comprise only the carbonate cap and slope facies sediments. A probable explanation could be the age and type of deformation: folding, faulting, strike-slipping, etc., which are typical of accretion and collision processes accompanied by continent rotation (Buslov et al., 2001; Sennikov et al., 2003; Buslov et al., 2004b). It is quite probably that chert sequences are less stable under folding and therefore have been preserved in old and strongly deformed accretionary complexes or buried beneath the latter. Nevertheless, the lithological association of pillow basalt, limestone, chert, siliceous shale and detrital turbidites is indicative of an intra-oceanic or oceanic island setting of rock formation.

One of the main problems which arises when reconstructing oceanic sequences, geodynamic settings and the evolution of oceanic magmatism, is determining the age of basalt-sedimentary units. So far, the main reliable method for obtaining age constrains for plume-related basalts is biostratigraphic analysis of microfossils contained in limestone and chert sequences which have conformable contacts with the basalts. The age of the limestone directly overlying basalt is closer to the age of seamount (i.e., basalt upper age boundary), whereas the age range of radiolarian chert associated with both limestone and basalt can be much wider. These may have been formed prior to, during and after formation of limestone-capped seamounts. The youngest rocks of OPS are usually terrigenous trench and slope facies: siliceous shale, mudstone, turbidite, clastic varieties marking the event of accretion. For example, the youngest faunal assemblages of the Taukha AC (Late Jurassic–Early Cretaceous) have been found in the sandstone and siliceous mudstone of two accretionary units of the Taukha AC: Kavalerovo and Dal'negorskiy (Khanchuk et al., 1989a; Golozubov et al., 1992). Therefore, the most reliable information about the age of volcanism can be obtained from the biostratigraphic data on limestones of carbonate cap and slope facies, which, unlike chert and siliceous shale, directly overlie the oceanic island/seamount.

Thus, the elements of OPS—OIB-type basalts, reef limestone, bedded radiolarian chert and terrifenous-clastic slopes facies are indicative of big oceanic realms existed in the geological past, which included zones of spreading and subduction on one hand and areas/chains of hot spot magmatism on the other.

4.2. Criteria for identification of intraplate basalts

Identification of OIB in accretionary complexes seems to be of special importance because in past decades such complexes were sometimes erroneously regarded as island-arc basalts or ophiolites (MORB). Now it is possible to differentiate island-arc basalts, MORB and OIB due to more precise determination of trace element and isotopic ratios, mainly based on inter-element relationships in the LREE–Th–Nb system. Although geochemical characteristics are useful in the assessment of original tectonic setting of basalts, they should not be the only means. In this section, therefore, the focus will not only be on chemical characteristics, but also on geological features that are typical of OPS units hosted by accretionary complexes. The criteria, both geological and geochemical, proposed for identification of oceanic islands, seamounts and plateaus associated with oceanic sediments can be as follows.

1. Occurrence of OPS units suggesting oceanic island setting: basalt, reef carbonate, clastic terrigenous-carbonate-siliceous slope facies, oceanic bottom chert (Figs. 5, 7 and 12).
2. Basalts occur as thick bodies of paleooceanic islands capped with carbonates (Fig. 12).
3. Thinner lava flows (up to 10 m) intercalated with siliceous shale, mudstone, carbonate breccia, etc., i.e., slope facies sediments.
4. Slope facies possess signatures of their sliding down the volcano slopes: synsedimentary or Z-folding, brecciation, variable thickness of beds.
5. Medium to high TiO_2 (>1.5 wt.%) and Al_2O_3/TiO_2 between 4 and 10 compared to 15 to 25 in island-arc basalts and 10 to 15 in MORB (Figs. 9, 11A; Table 3).
6. Medium to high LREE (La/Sm_n>1.3) and low to high degree of HREE differentiation: Gd/Yb_n can vary from 1.0 in younger seamounts and plateau basalts to 3 in Hawaiian-type OIB's (Mahoney et al., 1993; Regelous et al., 2003; Table 3; Fig. 11A).
7. High Nb contents or positive Nb anomalies relative to La and Th resulting in Nb/La_{pm}>1 and Nb/Th_{pm}>1; plateau basalts may have lower concentrations of Nb, however, unlike IAB, they are less enriched in Th and have Th/Nb_{pm}<La/Nb_{pm} (Figs. 10, 11B).
8. OPS units are spatially associated with nappe-thrust structures typical of accretionary complexes and include turbidite, ophiolites and high-pressure rocks of the blueschist and eclogite metamorphic facies. In some areas the accretionary tectonics are accompanied by strike-slip deformation resulting in formation of linear zones with re-oriented primary structures and steeply dipping imbricate structures (Buslov et al., 2001, 2004b).
9. OIB-type basaltic units, occurring within the same AC, may have different ages, because they were parts of seamount chains, created when oceanic plates move over mantle plumes, which record lavas erupted above a single plume over time (Regelous et al., 2003; Safonova, 2008).

4.3. Geochemical variability of intraplate basalts

In many respects oceanic islands and seamounts are the smaller equivalents of oceanic plateaus, in this section only geochemical features typical of the studied OIB's will be considered. Although the upwelling rates of magmatic melts, which produced oceanic islands, seem to be significantly lower that those suggested for oceanic plateaus, there is a continuous link between both. The mode of eruption, island, seamount or plateau, depends on the melt flow velocity and lithosphere thickness (e.g., Regelous et al., 2003 and the references therein; Maruyama et al., 2007). Hot spot magmatism produced chains of seamounts and islands, which typically have bimodal volcanism, mainly represented by basalts and rhyolites and associated pyroclastic rocks. Nevertheless, most of oceanic hot spots are dominated by basalts, enriched in incompatible trace elements and highly differentiated or depleted HREE signatures suggesting deep melting within the garnet stability field (Table 3; Figs. 10 and 11a). Although normal OIB's are enriched in incompatible trace elements and show evidence of melting within depths of garnet stability, there are lavas possessing flat REE patterns, indicative of shallower depth and/or higher degrees of melting (e.g., Sun, McDonough, 1989; Weaver, 1991; Hofmann, 1997; Polat et al., 1999; Regelous et al., 2003; Safonova, 2008; Table 3; Fig. 10). The majority of basaltic units from Paleo-Asian Ocean and Paleo-Pacific Ocean accretionary complexes are dominated by lavas with trace element enriched signatures (high La/Sm_n, Gd/Yb_n and low Zr/Nb), therefore an oceanic island/seamount setting should be suggested rather than a plateau.

The trace element and isotope compositions of the lavas erupted over one hot spot can vary with the age of the underlying oceanic lithosphere at the time of seamount magmatism. By analogy with the Emperor–Hawaii Seamount Chain (Regelous et al., 2003) the temporal compositional changes in the Paleo-Asian Ocean magmatism can be explained by variable degrees of melting of a heterogeneous mantle and variable lithosphere thickness. When the plume was situated beneath younger and thin oceanic lithosphere (at 600 Ma), melting produced Kurai melts with relatively depleted trace element compositions due to higher melting column, higher degrees of melting and, therefore, higher contribution of more refractory depleted source material. In contrast, younger Katun' lavas built on older and thicker crust (at 550 Ma), were produced by smaller degrees of melting, and consequently melts had greater contribution from incompatible-element-rich, easily melted materials of mantle heterogeneities (Safonova, 2008). Such a tendency seems to be a very useful indicator for the future geodynamic and petrologic modeling of Paleo-Asian Ocean and Paleo-Pacific Ocean intraplate magmatism. But to expand that kind of interpretation to the other localities of Paleo-Asian Ocean and Paleo-Pacific Ocean intraplate basalts we need not only good quality trace element data, but well-dated basaltic units, e.g., those overlain with fossil-bearing limestones, which can be reliably characterized in terms of biostratigraphy (Fig. 12).

4.4. The ~100 Ma time gap of the PAO intraplate magmatism

Fig. 13 shows the ages of basaltic units and accretionary complexes. The intraplate magmatism of the Paleo-Asian and Paleo-Pacific oceans was active from the Late Neoproterozoic to the Late Jurassic (600 to 140 Ma). After the Late Jurassic intraplate magmatism was active in the Pacific Ocean. Probably the oldest seamounts of the Emperor Chain of the Pacific Ocean (Early Cretaceous) were accreted to Eastern Kamchatka accretionary complexes in the Late Cretaceous (Saveliev, 2003). Younger active volcanoes on the Hawaiian Islands represent the current site of intraplate volcanism which, over the past 85 Ma has built the Hawaiian–Emperor seamount chain in the northern Pacific Ocean. Thus, the intraplate oceanic magmatism was active during more than 600 Ma. According to different models, this intraplate oceanic magmatism was related to a Pacific superplume (e.g., Maruyama et al., 2007; Utsunomiya et al., 2007) or North-Asian superplume (Yarmolyuk et al., 2000) or it was initiated by several superplumes, which acted within a single "mantle hot field" (Dobretsov and Buslov, 2007). However, a Middle Ordovician–Middle Devonian time gap is apparent during in the manifestation of intraplate magmatism (Fig. 13). This gap may be explained by a 120 to 150 Ma mantle plume periodicity (Larson and Olson, 1991), although before and after the 100 Ma time gap the periodicity of the intraplate magmatism was about 50 Ma. Moreover, some authors suggested a 10 Ma periodicity of mantle plume magmatism (Coffin and Eldholm, 2001). The Late Neoproterozoic, Early Cambrian and Late Cambrian basalts of the Kurai, Katun and Zasur'ia ACs (ca. 600, 550 and 500 Ma, respectively) have been recorded before the gap. The Late Devonian, Late Carboniferous, Middle Permian and Middle Triassic basalts of the Char, Akiyoshi, Mino-Tamba and S. Chichibu ACs (approximately 370, 320, 270 and 220 Ma, respectively) have been recorded after the gap. Therefore, no other such long gaps have been recorded.

Another explanation for the approximate 100 Ma gap may be due to our limited knowledge on poorly preserved accretionary complexes in strongly deformed strike-slip zones of Central Asia formed along the margin of the Siberian continent during the Middle Paleozoic

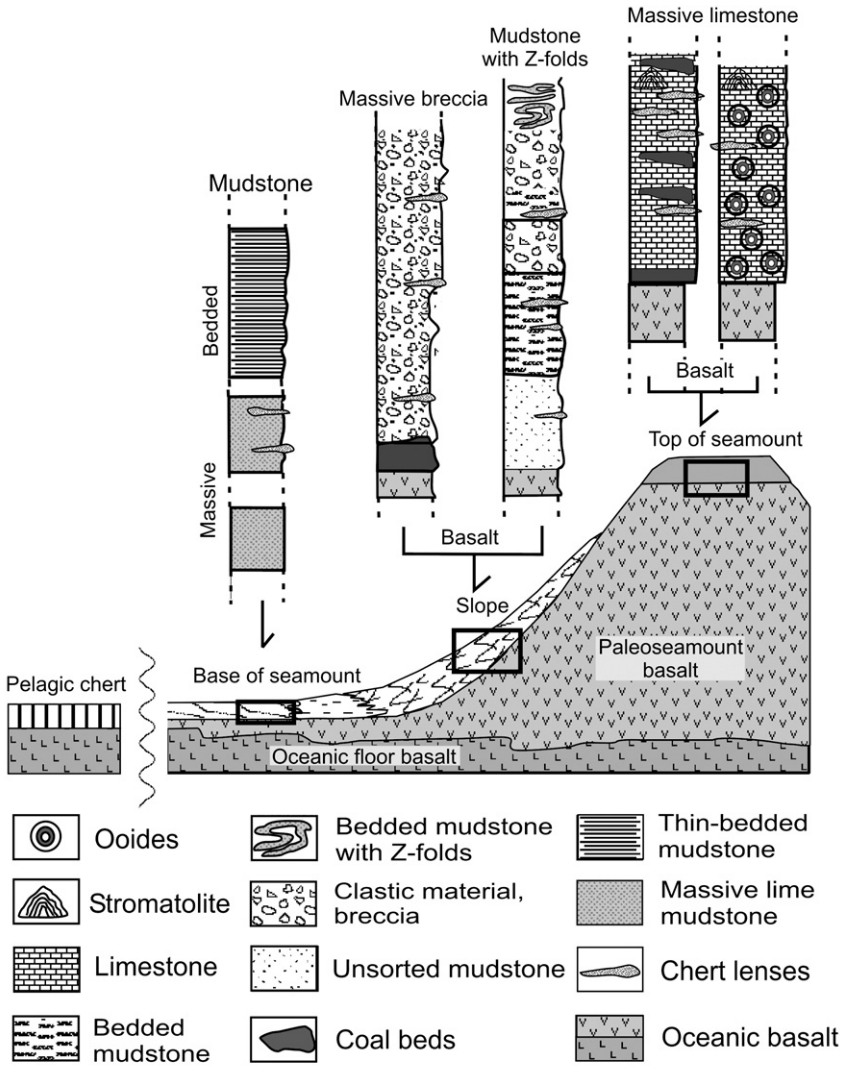

Fig. 12. Schematic reconstruction of a carbonate capped oceanic seamount based on real geological features of the Kurai and Katun' paleoseamounts (modified from Isozaki et al., 1990).

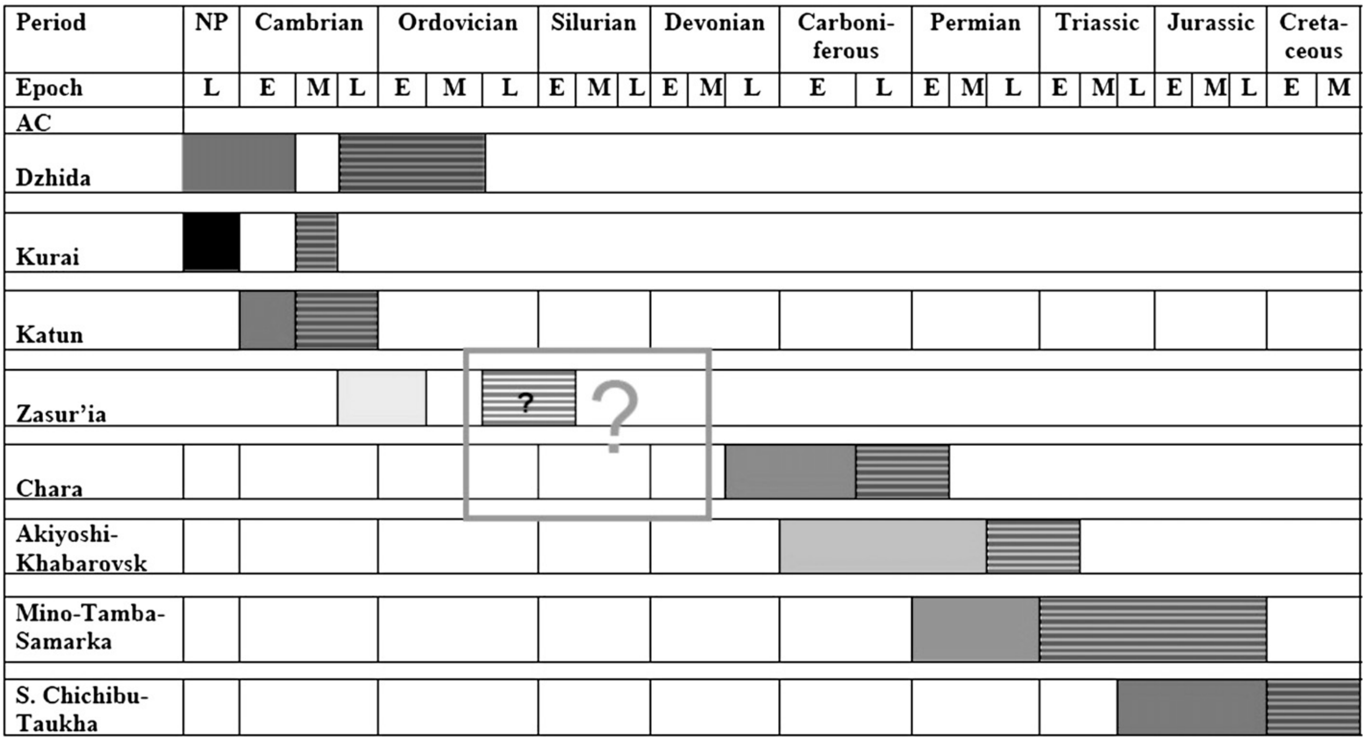

Fig. 13. Main periods of intraplate magmatism of the Paleo-Asian and Paleo-Pacific Ocean and the ages of basalt hosting accretionary complexes. NP—Neoproterozoic; AC—accretionary complex; quadrangles, filled—age of intraplate volcanism, striped—age of accretionary complex; E, M, L—early, middle, late, respectively.

(Buslov et al., 2004b). Moreover, most Central Asian ACs occur in areas which are sparsely populated and difficult to access. This makes their detailed study rather problematic and expensive. There is limited information about ophiolite-bearing accretionary complexes in Central Kazakhstan (Yakubchuk and Degtyarev, 1994), which may include Ordovician–Devonian OPS units and OIB-type basalts (A. Yakubchuk, pers. comm.), but no detailed geochemical data on OIB-type basalts and/or biostratigraphically dated OPS units have been reported. The Bayanhongor Ophiolite, Sulinheer and Zoolen ACs of Central and Southern Mongolia comprise OPS units of Late Neoproterozoic and Late Paleozoic age. Badarch et al. (2002) reported on Late Carboniferous–Early Permian clastic sediments and fossil-bearing limestone in the Sulinheer AC, Helo et al. (2006) about Lower Carboniferous marine limestone, chert, clastic sediments in the Zoolen AC of South-Central Mongolia, and Xiao et al. (2003) about Devonian fossil-bearing limestone, radiolarian chert, and siltstone in the Hegenshan AC of Inner Mongolia. However, no information about Middle Paleozoic OIB-type basalts closely associated with biostratigraphically characterized OPS units in Mongolia or China has so far been published. Should Middle Ordovician–Middle Devonian OPS units with OIB-type basalts be recognized in Kazakhstan and/or Mongolia, it would confirm the continuous character of the intraplate magmatism of the Paleo-Asian and Paleo-Pacific Ocean. Besides, this would contribute to our knowledge about the evolution of two oceans and the continental growth of Asia at the expense of not only accreted Gondwana-derived continental blocks, but also oceanic islands and seamounts. Moreover, detailed geochemical and petrologic study of intraplate basalts preserved in accretionary complexes would allow us to estimate driving forces of environmental change from the Late Neoproterozoic to Mesozoic and to evaluate the hypothesis that the Pacific superplume was significant for that change (Maruyama et al., 2007).

4.5. OPS-hosted mineral deposits

The Late Devonian to Early Carboniferous OIB-type basalts of the Char belt in East Kazakhstan and Carboniferous basalts of the Akioshi accretionary complex in Southwest Japan record an important event of mantle plume magmatism in the Paleo-Pacific Ocean and its related tectonic and metallogenic evolution of Central and East Asia. Island-arc volcanism and collisional granitic magmatism, which usually accompany and follow processes of accretion and collision, were responsible for formation of many mineral deposits. For example, most porphyry deposits of Kazakhstan formed during this time (Heinhorst et al., 2000). The accretionary complexes of Central Asia, Russian Far East and Japan host numerous polymetallic (i.e., Pb–Zn–Cu) and Mn deposits of Late Paleozoic and Early Mesozoic age. In the Central Asian Orogenic Belt, several large Cu–(Mo)–porphyry, Cu–Pb–Zn volcanic massive sulfide and intrusion-related Au deposits formed during both eras (Yakubchuk et al., 2001; Yakubchuk, 2004; Berzina, Sotnikov, 2007). Jurassic–Cretaceous magmatism in Russian Far East is considered to be prospective for porphyry Cu and epithermal Au mineralization (Goryachev and Yakubchuk, 2008).

Japanese accretionary complexes are known for two main types of mineral systems (Ohmoto, 1996; Watanabe et al., 1998): 1) Besshi-type base metal sulfide deposits mainly associated with Carboniferous–Permian basaltic lavas and tuffs and 2) stratiform manganese deposits associated with Middle Triassic–Jurassic bedded chert formed in an ocean basin environment, which is a common member of OPS and is often associated with intraplate basalts in accretionary complexes (Isozaki et al., 1990). The correct understanding of geodynamic evolution and tectonics is important for the explanation of the rich metal endowment of these regions, which is a result of a prolonged and complex history of ocean evolution, crustal growth and deformation in diverse tectonic settings. Therefore, the study of accretionary belts is important in terms of formation and localization of many commercially valuable deposits.

Thus, on one hand accretionary complexes comprise plume-related OPS intraplate basalts and sedimentary rocks, which are indicative of former big oceanic realms and may host stratiform manganese deposits (Koichiro et al., 2006), and on the other hand those basalts often occur in close association with ophiolites and other volcanic rocks hosting volcanic massive sulfide deposits (Solomon et al., 2004).

Chert-hosted bedded manganese deposits have been found within many accretionary complexes of Japan, e.g., the Gen-otani Mine of the Tamba area, Southwest Japan, the Karie mine in Ehime, the Otaniyama mine in the Kitakami Mountains, the Hirano mine on Oshima peninsula and smaller occurrences of Mn-enriched chert in the Inuyama area of the Mino area and at Shikoku, Southwest Japan (Nakae and Komuro, 2005 and the references therein). There are two alternative hypotheses on the origin of bedded manganese deposits: syngenetic and epigenetic. Nakae and Komuro (2005) argue that the Mn-bearing chert beds stratigraphically take an intermediate position between massive chert and upper bedded chert of the OPS succession, like at the Gen-otani Mine. Therefore, a syngenetic scenario for their origin seems to be more acceptable.

Similarly, Fe–Mn sedimentary ores of oceanic origin have been found in the Taukha accretionary complex, Russian Far East, which has a Jurassic age (Khanchuk et al., 1989a).

5. Conclusions

From our study of oceanic plate stratigraphy and intraplate magmatism of the Paleo-Asian and Paleo-Pacific Oceans, the following conclusions can be made.

(1) The intraplate basalts are associated with oceanic plate stratigraphy (OPS) units of the Paleo-Asian and Paleo-Pacific Oceans, which are hosted by the Early Cambrian to Late Cretaceous accretionary complexes of Altai-Sayan, Russian Far East and Southwest Japan. The OPS units of the two oceans have a number of features in common, the most important of which are as follows: (a) similar succession of oceanic sediments from pelagic chert to hemipelagic siliceous shales and carbonate breccia slope facies and to seamount cap reef carbonates; (b) intraplate basalts occur at the base of the sections and are usually overlain by carbonate “cap” sediments; (c) typical OIB-type chemistry of basalts is characterized by LREE–Nb–Ti enrichment. Some of the published trace element geochemical data was obtained by using the XRF method, which may result in significant analytical errors on such important elements as Nb and Th. Therefore, additional analytical studies of trace element geochemistry (by ICP MS) of the intraplate basalts hosted by the accretionary complexes of Russian Far East and Japan are necessary.

(2) Intraplate magmatism was active in the Paleo-Asian and Paleo-Pacific Oceans from the Late Neoproterozoic to the Early Cretaceous. However, there is a 100 Ma time gap in the evolution of the oceanic intraplate magmatism, which is probably a result of mantle plume periodicity or our insufficient knowledge of the OPS units hosted by accretionary complexes of Central Kazakhstan, Tien Shan and Central and Southern Mongolia.

(3) The study of intraplate magmatism and oceanic plate stratigraphy of paleo-oceans is very important because it is an integral part of the study of orogenic belts incorporating many commercially valuable mineral deposits. Identification of intraplate OPS units should be based on a combination and mutual correlation of geological, lithological and geochemical features of basalts and their associated sediments. OPS units, both magmatic and sedimentary, provide a geological record from the opening of paleo-oceans, to their subduction and formation of accretionary complexes, and finally to their closure accompanied by active tectonics, orogeny and ore mineralization.

Acknowledgments

The author is grateful to Prof. Buslov (IGM SB RAS, Novosibirsk) for many years of joint field work, research cooperation and permanent support of her studies. Prof. Satoru Kojima (University of Gifu, Japan), Dr. Satoshi Nakae (Geological Survey of Japan, AIST) and Dr. Marc Reichow (University of Leicester, UK) are thanked for useful discussions and constructive comments on the manuscript. The thorough reviews by anonymous reviewers are greatly acknowledged. I am grateful to Dr. Clare Davies (Woodside Energy Ltd., Australia), who provided me with English corrections of the manuscript. The work was partly supported by RFBR-JSPS international grant no. 07-05-91211.

References

Badarch, G., Cunningham, W.D., Windley, B.F., 2002. A new terrane subdivision for Mongolia: implications for the Phanerozoic crustal growth of Central Asia. Journal of Asian Earth Sciences 21, 87–110.

Berzina, A.P., Sotnikov, V.I., 2007. Character of formation of the Erdenet-Ovoo porphyry Cu–Mo magmatic center (northern Mongolia) in the zone of influence of a Permo–Triassic plume. Russian Geology and Geophysics 48, 141–157.

Bragin, N.Yu., 1991. Radiolarians and Lower Mesozoic Sequences of the Eastern USSR. Nauka, Moscow. 126 pp. (in Russian).

Bragin, N.Yu., 1992. Stratigraphy of Upper Paleozoic and Mesozoic units near Khabarovsk. Izvestija Akademii Nauk SSSR, Seria Geologicheskaya 2, 35–40 (in Russian).

Buslov, M.M., Safonova, I.Yu., Watanabe, T., Obut, O., Fujiwara, Y., Iwata, K., Semakov, N.N., Sugai, Y., Smirnova, L.V., Kazansky, A.Yu., 2001. Evolution of the Paleo-Asian Ocean (Altai-Sayan region, Central Asia) and collision of possible Gondwana-derived terranes with the southern marginal part of the Siberian continent. Geosciences Journal 5, 203–224.

Buslov, M.M., Fujiwara, Y., Iwata, K., Semakov, N.N., 2004a. Late Paleozoic–Early Mesozoic geodynamics of Central Asia. Gondwana Research 7, 791–808.

Buslov, M.M., Watanabe, T., Fujiwara, Y., Iwata, K., Smirnova, L.V., Safonova, I.Yu., Semakov, N.N., Kiryanova, A.P., 2004b. Late Paleozoic faults of the Altai region, Central Asia: tectonic pattern and model of formation. Journal of Asian Earth Sciences 23, 655–671.

Chen, C.-Y., Frey, F.A., Garcia, M.O., Dalrymple, G.B., Hart, S.R., 1991. The tholeiitic to alkaline basalt transition at Heleakala volcano. Maui, Hawaii. Contributions to Mineralogy and Petrology 106, 183–200.

Coffin, M.F., Eldholm, O., 2001. Large igneous provinces: progenitors of some ophiolites? In: Ernst, R.E., Buchan, K.L. (Eds.), Mantle Plumes: Their Identification through Time. Geological Society of America Special Paper, vol. 352, pp. 59–70.

Condie, K.C., 1994. Greenstones through time. In: Condie, K.C. (Ed.), Archean Crustal Evolution. Elsevier, Amsterdam, pp. 85–120.

Didenko, A.N., Mossakovskiy, A.A., Pecherskiy, D.M., Ruzhentsev, S.G., Samygin, S.G., Kheraskova, T.N., 1994. Geodynamics of Paleozoic oceans of Central Asia. Russian Geology and Geophysics 35 (7–8), 48–62.

Dobretsov, N.L., Vernikovsky, V.A., 2001. Mantle plumes and their geologic manifestations. International Geology Review 43, 771–787.

Dobretsov, N.L., Buslov, M.M., 2007. Late Cambrian–Ordovician tectonics and geodynamics of Central Asia. Russian Geology and Geophysics 48, 1–12.

Dobretsov, N.L., Berzin, N.A., Buslov, M.M., 1995. Opening and tectonic evolution of the Paleo-Asian Ocean. International Geology Review 37, 335–360.

Dobretsov, N.L., Buslov, M.M., Safonova, I.Yu., Kokh, D.A., 2004. Fragments of oceanic islands in the Kurai and Katun' accretionary wedges of Gorny Altai. Russian Geology and Geophysics 45, 1381–1403.

Golozubov, V.V., Khanchuk, A.I., Kemkin, I.V., Panchenko, I.V., Simanenko, V.P., 1992. Taukha and Zhuravlev terranes of the Southern Sikhote-Alin. Far East Geological Institute Publishing House, Vladivostok. 82 pp. (in Russian).

Gordienko, I.V., Filimonov, A.V., Minina, O.R., Gornova, M.A., Medvedev, A.Ya., Klimuk, V.S., Elbaev, A.L., Tomurtogoo, O., 2007. Dzhida island-arc system in the Paleoasian Ocean: structure and main stages of Vendian–Paleozoic geodynamic evolution. Russian Geology and Geophysics 48, 91–107.

Goryachev, N., Yakubchuk, A., 2008. Gold deposits of Magadan Region, northeastern Russia: yesterday, today and tomorrow. SEG Newsletter 74, 1–15.

Heinhorst, J., Lehmann, B., Ermolov, P., Serykh, V., Zhurutin, S., 2000. Paleozoic crustal growth of Central Asia: evidence from magmatic-hydrothermal ore systems of Central Kazakhstan. Tectonophysics 328, 69–87.

Helo, Ch., Hegner, E., Kroner, A., Badarch, G., Tomurtogoo, O., Windley, B.F., Dulski, P., 2006. Geochemical signature of Paleozoic accretionary complexes of the Central Asian Orogenic Belt in South Mongolia: constrains on arc environments and crustal growth. Chemical Geology 227, 236–257.

Hofmann, A.W., 1997. Mantle geochemistry: the message from oceanic volcanism. Nature 385, 219–229.

Hou, Z., Zaw, K., Pan, G., Mo, X., Xu, Q., Hu, Y., Li, X., 2007. Sanjiang Tethyan metallogenesis in S.W. China: tectonic setting, metallogenic epochs and deposit types. Ore Geology Reviews 31, 48–87.

Humphris, S.E., 1984. The mobility of the rare earth elements in the crust. In: Henderson, P. (Ed.), Rare Earth Element Geochemistry. Elsevier, Amsterdam, pp. 317–342.

Ichiyama, Yu., Ishiwatari, A., 2005. HFSE-rich picritic rocks from the Mino accretionary complex, southwestern Japan. Contributions to Mineralogy and Petrology 149, 373–387.

Ichiyama, Yu., Ishiwatari, A., Hirahara, Y., Shuto, K., 2006. Geochemical and isotopic constraints on the genesis of the Permian ferropicritic rocks from the Mino-Tamba belt, SW Japan. Lithos 89, 47–65.

Ishiwatari, A., Nakae, S., 2001. Yakuno ophiolite and greenstones of the Tamba belt in the Wakasa areas, Fukui prefecture. Excursion Guidebook, the 108th Annual Meeting, Geological Society of Japan, Kanazawa, pp. 67–84.

Isozaki, Y., 1997. Contrasting two types of orogen in Permo-Triassic Japan: accretionary versus collisional. Island Arc 6, 2–24.
Isozaki, Y., Maruyama, Sh., Fukuoka, F., 1990. Accreted oceanic materials in Japan. Tectonophysics 181, 179–205.
Iwata, K., Obut, O.T., Buslov, M.M., 1997a. Devonian and Lower Carboniferous radiolaria from the Chara ophiolite belt, East Kazakhstan. News of Osaka Micropaleontologist 10, 27–32.
Iwata, K., Sennikov, N.V., Buslov, M.M., Obut, O.T., Shokalsky, S.P., Kuznetsov, S.A., Ermikov, V.D., 1997b. Upper Cambrian–Early Ordovician age of the Zasur'ia basalt-chert-terrigenous formation (northwestern Gorny Altai). Russian Journal of Geology and Geophysics 38, 1427–1444.
Jahn, B.-M., Wu, F., Chen, B., 2000. Granitoids of the Central Asian Orogenic Belt and continental growth in the Phanerozoic. Transactions of the Royal Society of Edinburgh. Earth Sciences 91, 181–193.
Kanmera, K., Sano, H., Isozaki, Y., 1990. Akiyoshi terrane. In: Ichikawa, K., Mizutani, S., Hara, I., Hada, S., Yao, A. (Eds.), Pre-Cretaceous Terranes of Japan. Publication of IGCP Project: Pre-Jurassic Evolution of Eastern Asia No. 224, Osaka, pp. 49–62.
Khanchuk, A.I., Kemkin, I.V., 2003. Mesozoic geodynamic evolution of the Japan Sea Region. Vestnik DVO RAN 6, 94–108 (in Russian).
Khanchuk, A.I., Kemkin, I.V., Panchenko, I.V., 1989a. Geodynamic evolution of Sikhote-Alin and Sakhalin in Middle Paleozoic and Early Mesozoic. In: Scheglov, A.D. (Ed.), Pacific Margin of Asia: Geology. Nauka, Moscow, pp. 218–255 (in Russian).
Khanchuk, A.I., Nikitina, A.P., Panchenko, I.V., Buriy, G.I., Kemkin, I.V., 1989b. Paleozoic and Mesozoic guyots of Sikhote-Alin and Sakhalin. Doklady Akademii Nauk SSSR, 307, 186–190.
Kirillova, G.L., Natal'in, B.A., Zyabrev, S.V., Sakai, T., Ishida, K., Ishida, N., Ohta, T., Kozai, T., 2002. Upper Jurassic–Cretaceous deposits of East Asian continental margin along the Amur River. In: Kirillova, G.L., Natal'in, B.A., Zyabrev, S.V., Sakai, T., Ishida, K., Ishida, N., Ohta, T., Kozai, T. (Eds.), Upper Jurassic–Cretaceous deposits of East Asian continental margin along the Amur river. Field Excursion Guidebook, Khabarovsk, pp. 6–22.
Koichiro, F., Tatsuo, N., Takazumi, N., Kiyoko, K., Yasuhiro, K., 2006. Geochemistry and origin of Ananai Stratiform manganese deposit in the Northern Chichibu Belt, Central Shikoku, Japan. Resource Geology 56, 399–414.
Koizumi, K., Ishiwatari, A., 2006. Oceanic plateau accretion inferred from Late Paleozoic greenstones in the Jurassic Tamba accretionary complex, southwest Japan. Island Arc 15, 58–83.
Kojima, S., Kametaka, M., 2000. Jurassic accretionary complexes in East Asia. Memories of Geological Society of Japan 55, 61–72 (in Japanese with English abstract).
Kojima, S., Kemkin, I.V., Kametaka, M., Ando, A., 2000. A correlation of accretionary complexes of southern Sikhote-Alin of Russia and the Inner zone of southern Japan. Geoscience Journal 4, 175–185.
Kondo, N., Adachi, M., 1975. Mesozoic strata of the area north of Inuyama, with special reference to the Sakahogi conglomerate. Journal of Geological Society of Japan 81, 373–386.
Kovalenko, V.I., Yarmolyuk, V.V., Kovach, V.P., Budnikov, S.V., Zhuravlev, D.Z., Kozakov, I.K., Kotov, A.B., Rytsk, E.Yu., Salnikova, E.B., 1999. Crust-forming magmatic processes during formation of the Central Asian fold belt: Sm–Nd isotopic data. Geotektonika 3, 21–41 (in Russian).
Larson, R.L., Olson, P., 1991. Mantle plumes control magnetic reversal frequency. Earth and Planetary Science Letters 107, 437–447.
Li, J.-Y., 2006. Permian geodynamic setting of Northeast China and adjacent regions: closure of the Paleo-Asian Ocean and subduction of the Paleo-Pacific Plate. Journal of Asian Earth Sciences 26, 207–224.
Ludden, J., Gelinas, L., Trudel, P., 1982. Archean metavolcanics from the Rouyn-Noranda district, Abitibi greenstone belt, Québec. 2. Mobility of trace elements and petrogenetic constrains. Canadian Journal of Earth Science 19, 2276–2287.
Mahoney, J.J., Storey, M., Duncan, R.A., Spencer, K.J., Pringle, M., 1993. Geochemistry and geochronology of Leg130 basement lavas: nature and origin of the Ontong Java Plateau. Proceedings of the Ocean Drilling Program. Scientific Results 130, 3–22.
Maruyama, Sh., 1994. Plume tectonics. Journal of Geological Society of Japan 100, 24–49.
Maruyama, Sh., Isozaki, Yu., Kimura, G., Terabayashi, M., 1997. Paleogeographic maps of the Japanese Islands: plate tectonic synthesis from 750 Ma to the present. Island Arc, 6, 121–142.
Maruyama, Sh., Yuen, D.A., Windley, B.F., 2007. Dynamics of plumes and superplumes through time. In: Yuen, D.A., Maruyma, Sh., Karato, Sh., Windley, B.F. (Eds.), Superplumes. Springer, the Netherlands, pp. 441–502.
Matsuoka, A., 1992. Jurassic–Early Cretaceous tectonic evolution of the Southern Chichibu terrane, Southwest Japan. Paleogeography, Paleoclimatology, Palaleoecology 96, 71–88.
Matsuoka, A., Yao, A., 1990. Southern Chichibu Terrane. In: Ichikawa, K., Mizutani, Sh., Hara, I., Hada, Sh., Yao, A. (Eds.), Publication of IGCP Project: Pre-Jurassic Evolution of Eastern Asia No. 224, Osaka. Pre-Cretaceous Terranes of Japan, pp. 203–216.
McDonough, W.F., Sun, S.-S., 1995. The composition of the Earth. Chemical Geology 120, 223–253.
Mizutani, Sh., Kojima, S., 1992. Mesozoic radiolarian biostratigraphy of Japan and collage tectonics along the eastern continental margin of Asia. Paleogeography, Paleoclimatology, Palaleoecology 96, 3–22.
Montelli, R., Nolet, G., Dahlen, F.A., Masters, G., Engdahl, E.R., Hung, S.-H., 2004. Finite-frequency tomography reveals a variety of plumes in the mantle. Science 303, 338–343.
Morgan, W.J., 1971. Convection plumes in the lower mantle. Nature, 230, 42–43.
Nakae, S., 2000. Regional correlation of the Jurassic accretionary complex in the Inner Zone of Southwest Japan. Memories of Geological Society of Japan 55, 73–98 (in Japanese with English abstract).
Nakae, S., Komuro, K., 2005. Radiolarian age of chert-hosted bedded manganese deposits from the Gen-otani mine of the Tamba district, Northern Kyoto City, Japan. Resource Geology 55, 311–320.
Noda, M., 1956. Stratigraphical studies of the Carboniferous and Permian systems in Manchuria. Reports on Earth Science, Department of General Education, Kyushu University, no. 3, pp. 1–73.
Nolet, G., Allen, R., Zhao, D.-P., 2007. Mantle plume tomography. Chemical Geology 241, 248–263.
Ohmoto, H., 1996. Formation of volcanogenic massive sulfide deposits. Ore Geology Reviews 10, 135–177.
Onoue, T., Nagai, K., Kamishima, A., Seno, M., Sano, H., 2004. Origin of basalts from Sambosan accretionary complex, Shikoku and Kyushu. Journal Geological Society, Japan 110, 222–236 (in Japanese with English abstract).
Parfenov, L.M., Bulgatov, A.N., Gordienko, I.V., 1995. Terranes and accretionary history of the Transbaikal orogenic belts. International Geology Review 37, 736–751.
Polat, A., Kerrich, R., Wyman, D., 1999. Geochemical diversity in oceanic komatiites and basalts from the late Archean Wawa greenstone belts, Superior Province, Canada: trace element and Nd isotope evidence for a heterogeneous mantle. Precambrian Research 94, 139–173.
Regelous, M., Hofmann, A.W., Abouchami, W., Galer, S.J.G., 2003. Geochemistry of lavas from the Emperor Seamounts, and the geochemical evolution of Hawaiian magmatism from 85 to 42 Ma. Journal of Petrology 44, 113–140.
Repina, L.N., Romanenko, E.V., 1964. Trilobites and Lower Cambrian stratigraphy of Altai-Sayan folded area. Nauka, Moscow. 74 pp. (in Russian).
Ruzhentsev, S.V., Minina, O.R., Aristov, V.A., Katyukha, Yu.P., Golionko, B.G., 2005. Tectonics of the Ikat-Bagdara and Dzhida zones of Western Transbaikalia. In: Leonov, M.G. (Ed.), Tectonics of Central Asia. GEOS, Moscow, pp. 171–196 (in Russian).
Safonova, I.Yu., 2005. Vendian–Paleozoic basalts of the Paleo-Asian Ocean incorporated in foldbelts of Gorny Altai and East Kazakhstan: geodynamic settings of formation. Cand. Sci. Thesis Autoreferate. NP AI «Geo», Novosibirsk, 20 pp. (in Russian).
Safonova, I.Yu., 2008. Geochemical evolution of the Paleo-Asian Ocean intra-plate magmatism from the Late Neoproterozoic to the Early Cambrian. Petrology 16, 492–511.
Safonova, I.Yu., Buslov, M.M., Iwata, K., Kokh, D.A., 2004. Fragments of Vendian–Early Carboniferous oceanic crust of the Paleo-Asian Ocean in foldbelts of the Altai-Sayan region of Central Asia: geochemistry, biostratigraphy and structural setting. Gondwana Research 7, 771–790.
Safonova, I.Yu., Simonov, V.A., Buslov, M.M., Ota, T., Maruyama, Sh., 2008. Neoproterozoic basalts of the Paleo-Asian Ocean (Kurai accretion zone, Gorny Altai, Russia): geochemistry, petrogenesis, geodynamics. Russian Geology and Geophysics 49, 254–271.
Sano, H., Kanmera, K., 1991. Collapse of ancient oceanic reef complex—what happened during collision of Akiyoshi reef complex? Sequence of collisional collapse and generation of collapse products. Journal Geological Society, Japan 97, 631–644.
Sano, H., Kojima, S., 2000. Carboniferous to Jurassic oceanic rocks of Mino-Tamba-Ashio terrane, southwest Japan. Memories of Geological Society of Japan 55, 123–144 (in Japanese with English abstract).
Sano, S., Hayasaka, Y., Tazaki, K., 2000. Geochemical characteristics of Carboniferous greenstones in the Inner Zine of Southwest Japan. Island Arc 9, 81–96.
Saveliev, D.P., 2003. Within-plate alkali basalts of the Cretaceous accretionary complex (Eastern Kamchatka). Volcanology and Seismology 1, 14–20 (in Russian).
Scotese, C.R., McKerrow, W.S., 1990. Revised world maps and introduction. In: McKerrow, W.S., Scotese, C.R. (Eds.), Paleozoic Paleogeography and Biostratigraphy. Geology Society London, Memoir, vol. 12, pp. 1–21.
Sengör, A.M.C., Natal'in, B.A., Burtman, V.S., 1993. Evolution of the Altaid tectonic collage and Palaeozoic crustal growth in Eurasia. Nature 364, 299–307.
Sennikov, N.V., Iwata, K., Ermikov, V.D., Obut, O.T., Khlebnikova, T.V., 2003. Oceanic sedimentation settings and fauna associations in the Paleozoic on the southern framing of the West Siberian Plate. Russian Geology and Geophysics 44 (1–2), 156–171.
Shevelev, E.K., 1987. Age of volcanogenic-siliceous-terrigenous sediments of the basement of the Middle-Amur basin. Pacific Geology 3, 13–16 (in Russian).
Solomon, M., Tornos, F., Large, R.R., Badham, J.N.P., Both, R.A., Zaw, Khin, 2004. Zn–Pb–Cu volcanic-hosted massive sulphide deposits: criteria for distinguishing brine pool-type from black smoker-type sulphide deposition. Ore Geology Reviews 25, 259–283.
Sun, S., McDonough, W.F., 1989. Chemical and isotopic systematics of oceanic basalts: Implications for mantle composition and processes. In: Saunders, A.D., Norry, M.J. (Eds.), Magmatism in the Ocean Basins. Geological Society of London, Special Publication, vol. 42, pp. 313–345.
Suzuki, N., Kojima, S., Kano, H., Yamakita, S., Misaki, A., Ehiro, M., Otoh, Sh., Kurihara, T., Aoyama, M., 2005. Permian radiolarian faunas from chert in the Khabarovsk Complex, Far East Russia, and the age of each lithological unit of the Khabarovsk complex. Journal of Paleontology 79 (4), 686–700.
Tatsumi, Y., Kani, T., Ishizuka, H., Maruyama, Sh., Nishimura, Yu., 2000. Activation of Pacific mantle plumes during the Carboniferous: evidence from accretionary complexes in southwest Japan. Geology 28, 580–582.
Taylor, S.T., McLennan, S.M., 1985. The Continental Crust: Composition and Evolution. Blackwell, Oxford. 312 pp.
Terleev, A.A., 1991. Stratigraphy of Vendian–Cambrian sediments of the Katun anticline (Gorny Altai). In: Khomentovskiy, V.V. (Ed.), Late Precambrian and Early Paleozoic of Siberia. UIGGM Publishing, Novosibirsk, pp. 82–106 (in Russian).
Uchio, Y., Isozaki, Yu., Ota, T., Utsunomiya, A., Buslov, M., Maruyama, Sh., 2004. The oldest mid-oceanic carbonate buildup complex: setting and lithofacies of the Vendian (Late Neoproterozoic) Baratal limestone in the Gorny Altai Mountains, Siberia. Proceedings of the Japan Academy 80, 422–428.
Utsunomiya, A., Ota, T., Windley, B.F., Suzuki, N., Uchio, Y., Munekata, K., Maruyama, Sh., 2007. In: Yuen, D.A., Maruyma, Sh., Karato, Sh., Windley, B.F. (Eds.), Superplumes. Springer, the Netherlands, pp. 363–408.
Volokhin, Yu.G., Buriy, G.I., Rudenko, V.S., Filippov, A.N., 1990. Triassic chert formation of the Southern Sikhote-Alin. Izvestija Akademii Nauk SSSR, Seria Geologicheskaya 4, 45–57 (in Russian).

Wakita, K., 2000. Melanges of the Mino Terrane. Memories of Geological Society of Japan 55, 145–163 (in Japanese with English abstract).
Wakita, K., Metcalfe, I., 2005. Ocean plate stratigraphy in East and Southeast Asia. Journal of Asian Earth Sciences 24, 679–702.
Watanabe, M., Nishido, H., Hoshino, K., Hayasaka, Y., Imoto, N., 1998. Metallogenic epochs in the Inner Zone of southwest Japan. Ore Geology Reviews 12, 267–288.
Weaver, B.L., 1991. The origin of ocean island basalts and member compositions: trace element and isotopic constrains. Earth and Planetary Science Letters 104, 381–397.
Winchester, J.A., Floyd, P.A., 1977. Geochemical discrimination of different magma series and their differentiation products using immobile elements. Chemical Geology 20, 325–343.
Windley, B.F., Alexeiev, D., Xiao, W., Kroner, A., Badarch, G., 2007. Tectonic models for accretion of the Central Asian Orogenic Belt. Journal of the Geological Society of London, 164, 31–47.
Xiao, W., Windley, B.F., Hao, J., Zhai, M., 2003. Accretion leading to collision and the Permian Solonker suture, Inner Mongolia, China: termination of the Central Asian orogenic belt. Tectonics 22, 1–20.
Yakubchuk, A.S., 2004. Architecture and mineral deposit settings of the Altaid orogenic collage: a revised model. Journal of Asian Earth Sciences 23, 761–779.
Yakubchuk, A.S., Degtyarev, K.E., 1994. The remnants of the Paleo-Asian Ocean within Central Kazakhstan. In: Coleman, R.G. (Ed.), Reconstruction of the Paleo-Asian Ocean, Proceedings, 29th International Geological Congress, Part B, VSP BV, Netherlands, pp. 7–24.
Yakubchuk, A.S., Seltmann, R., Shatov, V.V., Cole, A., 2001. The Altaids: tectonic evolution and metallogeny. Society of Economic Geologists Newsletter 46, 7–14.
Yarmolyuk, V.V., Kovalenko, V.I., Kuz, 'min, M.I., 2000. North-Asian Superplume during the Phanerozoic: magmatism and deep geodynamics. Geotektonika 5, 3–29 (in Russian).
Zonenshain, L.P., 1973. The evolution of central Asiatic geosynclines through sea-floor spreading. Tectonophysics 19, 213–232.